Low Temperature Elastic and Electronic Properties of MAX Phases

A Thesis

Submitted to the Faculty

of

Drexel University

by

Peter Finkel

in partial fulfillment of the

requirements for the degree

of

Doctor of Philosophy

June 2003

Dedications

To my parents

Acknowledgments

It is a great honor to me to express my gratitude to my advisor Dr.Michel Barsoum for his interest to my research, encouragement, continuous scientific and educational support, inspiration and enthusiasm toward my work. I have been very fortunate to learn from him so much working on my thesis. I would like to thank Dr. Jeffrey Hettinger and Dr. Sam Lofland, Rowan University, for valuable collaboration and helping me to interpret experimental results, invaluable discussions, great suggestions and for their willingness to put aside an appreciable amount of time to review the results and interest in reviewing this thesis and participating in my defense committee. I would like specially to thank Dr. Somdev Tyagi and Dr. Yury Gogotsi for the time and interest in reviewing this thesis and participating in my defense committee. Author is also very grateful to Prof. Jean Toulouse of Lehigh University for allowing us to use his equipment and helpful suggestions and providing me with technical support in area of ultrasonics.

I also would like to express my gratitude to all people and colleagues I had an opportunity to collaborate during my work on PhD Thesis. My special thanks to: Dr. Tamer El-Raghy, and all students and faculty of the Materials Engineering Department, Drexel University, for help in analysis of experimental results, valuable discussions and suggestions and specimen' preparation; Mrs. Judy Trachtman from Drexel University, for her great help in solving administrative problems, friendly advice and support. I would like to thank my first graduate advisor Dr.Y.Bogod from the Institute for Low Temperature Physics, Academy of Science of Ukraine for

introducing me to the so exciting and wonderful world of Physics and Materials Science. Special thanks is to Physical Acoustic Corp for using their equipment and Thomson Consumer Electronics and TTW Lancaster R&D Center for sponsoring my research and giving me the opportunity to finish this work.

Finally, I would like to thank my family for their understanding, help and encouragement, and especially to my father for his mentoring, intellectual support and advice. I believe without this support this work would not be possible.

Table of Contents

List of Tables

List of Figures

Abstract

Low Temperature Elastic and Electronic Properties of MAX Phases

Peter Finkel

Michel Barsoum, Ph.D.

The $M_{n+1}AX_n$ phases (where M is an early transition metal, A is an A-group element and, X is C and/or N and n = 1 to 3) represent a new class of carbides and nitrides and can be best described as polycrystalline nanolaminates. They combine some of the best properties of ceramics and metals. Their physical properties (stiffness, damage and thermal shock resistance, high thermal and electrical conductivity) along with the fact they are readily machinable, make them extremely attractive in terms of the potential technological applications. Knowledge of low-temperature behavior is vital because it can provide insight into $M_{n+1}AX_n$-phases' physical properties. This work entails the systematic study of the elastic, electrical, galvanomagnetic and thermal properties of these materials in the 4-300 K temperature range.

The elastic constants of these compounds (Ti_3SiC_2, Ti_3AlC_2 and Ti_4AlN_3) were measured over the 20-300 K temperature range. Their Young's and shear modulii determined from ultrasonic velocities were in 300-335 and 124-140 GPa range, respectively; both moduli increase slowly with decreasing temperature and reaching a maximum at temperatures below 125 K; Poisson's ratio is 0.2. The Debye temperatures, θ_D, of these compounds calculated from the mean ultrasonic velocity are in 650-780K range which is in agreement with data obtained from low-temperature heat capacity measurements.

To characterize the electronic transport properties, the resistivity, magnetoresistance, Hall effect, Seebeck coefficient and magnetic susceptibility were measured in the 4-300K range, and in magnetic fields up to 9T. All MAX-phases exhibit metal-like temperature dependence of the resistivity $\rho(T)$. θ_D for most of the MAX-phases determined by fitting $\rho(T)$ with the Bloch T^5 formula were in good agreement with the values determined from elastic and calorimetric measurements. The carrier density of electrons *n* (or holes, *p*) and their mobilities were calculated utilizing a semi-classical isotropic two-band model. It was shown that most of the $M_{n+1}AX_n$ (n=2) phases (Ti_3SiC_2, Ti_3AlC_2, Ti_3GeC_2) are nearly compensated conductors with $n \sim p$ and total density of electrons and holes of $\sim 10^{28}$ m^3. This result also was is in agreement with conclusions based on negligible thermopower of these solids. Extensive study of electronic and galvanomagnetic properties and analysis of the results suggest $M_{n+1}AX_n$ (n=2) phases can be characterized by relatively high charge carrier mobilities.

1. Introduction

1.1 Background

There is a need for new materials that have high strength, large modulus, are corrosion resistant, and, at the same time, can retain all these properties over a broad temperature range, and be usable from cryogenic to refractory environment. Material scientists continue a search for new low and high temperature tolerant materials that can be easily machined, light-weight, tough, highly reliable with the potential to be used in different environments: from large-scale aerospace applications, combustion engines, power plants to electronic device applications in the semiconductor industry and microelectronics. It is well known that there are special metal alloys developed which are capable of sustaining favorable properties to temperatures up to 1000 ^{o}C. Ceramics can work to significantly higher temperatures. However, being stiff and hard, they are very generally brittle and difficult to machined, and, furthermore, are not generally thermal shock tolerant. In spite of significant progress over the past several decades, the wide application of ceramics is still limited.

In 1996, there was remarkable breakthrough in this area, when Barsoum and El-Raghy and their research group from Drexel University reported the successful synthesis of fully dense, single phase Ti_3SiC_2. This compound structurally resembles the Hägg phases (so called, H-phases) discovered in the sixties. This class of materials was lately named MAX phases because of their chemistry: they all are ternary layered hexagonal carbides and nitrides, with the general formula $M_{n+1}AX_n$,

where n =1 to 3, M is an early transition metal, A is an A-group element and X is either C and/or N. It has been shown that Ti_3SiC_2 exhibits large thermal and electrical conductivities, structural stability up to 1700 ^oC in inert atmospheres, high fracture toughness, good damage tolerance, shock resistance, good oxidation properties and low coefficient of friction, and yet, it is readily machinable.

So far possible applications of these material are already identified and some of them have been the subjects of patents. It is anticipated that the MAX-phase materials will be used in many different applications ranging from tribology to electrical contacts at high temperatures. For instance, used as substrates, the $M_{n+1}AX_n$ phases, possibly coupled with buffer layers, could be ideal for an array of electronic devices. Their high thermal conductivity allows rapid dissipation of heat from devices and their structural stability, together with their large electrical conductivities can function as ground planes and electrical shields. There are many other applications, brushes in electric motors being the most obvious, that can take advantage of this combination of properties.

This technological interest triggered a round of theoretical and experimental research aimed to better understand their nature and physics.

In this thesis we report a comprehensive experimental characterization and analysis of the elastic and electrical properties of some of these novel material. The main results of this thesis are contained in the four published papers [1-4] and another manuscript that has been prepared for submission.

This thesis starts with a literature review that focuses on the history of the MAX phases and their properties. This review attempts to identify the important

properties of the MAX phases known prior to the initiation of this work the motivation of this thesis.

The overall thesis is divided into two parts. First, Chapter 2, is devoted to the results of elastic constants measurements, while Chapters 3-5 concentrate on electronic and galvanomagnetic properties. The natural internal chronological order has been maintained, that could help the reader to gradually learn about the low temperature physical properties of MAX phases. The reader should be aware that the order of the measurements was strongly influenced by the order of the availability of high quality materials.

The elastic constants (first part) are some of the most fundamental quantities to be evaluated since they link the interatomic bonding energy with the structural and thermal properties of the material. Chapter 2 contains the first reported values of Young's, shear and bulk moduli of predominantly single phase samples of Ti_3SiC_2 measured nondestructively. In this work the moduli were measured as a function of temperature in the 50-300K range. Elastic constants were determined by means of ultrasonic pulse velocity measurements with a phase sensitive detection technique. The temperature dependence of the elastic constants was fitted to an appropriate theoretical function. Chapter 2 also deals with the results of elastic properties measurements on Ti_3AlC_2, and Ti_4AlN_3. One of the more important results of this chapter is the extraction of the Debye temperatures of these phases from the ultrasonic velocities. The values of these measurements are shown to correlate well with results obtained from specific heat experiments and theoretical calculations.

Chapters 3-6 discuss the results of the electric and transport properties of Ti_3SiC_2 [3], Ti_3AlC_2, and Ti_4AlN_3 [4] , as well as Ti_3 (Si,Ge)C_2 solid solutions. Ref. 3 describes the electronic and galvanomagnetic results for Ti_3SiC_2, and it is reproduced in Chapter 3 nearly as it appeared in the Physical Review B. Chapter 4 reports transport results for Ti_3AlC_2 and Ti_4AlN_3. Chapter 5 contains the first results of the elastic and transport measurements of the solid solutions on A-site compounds, namely Ti_3(Si,Ge)C_2. In future work the properties of other group of ternary carbides and nitrides, such as Ti_2AlC, Ti_2AlN, V_2AlC, Nb_2AlC, Cr_2AlC and Ti_2GeC among others will be measured in order to study the effect of composition on the physical and electronic properties in these isostructural compounds. The general conclusion chapter recapitulates the important results and their implications. Finally, Appendix C outlined the experimental ultrasonic elastic constants measurements technique. Additional details regarding this method which were not included into Chapter 2 but will also be described in Appendix C.

1.2 An Overview of the Physical Properties of the MAX Phases

Recently it has been shown that the MAX phases are best described as thermodynamically stable polycrystalline nanolaminates that, surprisingly, exhibit both metallic and ceramic features [5]. Some of them (e. g. Ti_3SiC_2, Ti_3AlC_2 and Ti_4AlN_3) are elastically quite stiff but despite the high stiffness they are readily machinable. Most of them are excellent conductors of electricity and heat; the thermal and electrical conductivities of Ti_3SiC_2 are more than double those of Ti

metal. To date, around 25 of the roughly more than 50 known $M_{n+1}AX_n$ phases have been synthesized. To date the physical properties of only few of them have been fully characterized.

The history of these materials started forty years ago when Nowotny and Jeitschko [7] discovered that the vast majority of these ternary carbides and nitrides. At the time, the 211's were labeled the H-phases, because they have a chemistry of the form M_2AX; their unit cell is hexagonal and they are made of layers of M_2X separated by layers of pure A. The same group discovered Ti_3SiC_2 in 1967 [8]. It was also related to the H-phases because its unit cell made of layers of Ti_3C_2 between pure layers of Si. In general, all these phases are hexagonal (space group $P6_3/mmc$) and layered, wherein pure layers of the A-group elements are interleaved with $M_{n+1}X_n$ layers consisting of octahedral unit blocks identical to the ones in the rock-salt structure [8].

Recently an updated list shows that there are more than 50 M_2AX, or 211 compounds, three M_3AX_2 or 312 compounds (Ti_3SiC_2, Ti_3GeC_2, Ti_3AlC_2) and one M_4AX_3 or 413 compound, Ti_4AlN_3. These ternaries are hexagonal with c/a ratios in the range of 3-6 [9]. In the 312 compounds the *c*-axis stacking sequence includes double layers of distorted edge sharing CTi_6 octahedra, reminiscent of the TiC structure. The double layers are separated by sheets of hexagonal nets of the A-group element. In case of the 413 compounds there are three A-group element layers separated.

This layered structure of the MAX phases gives rise to a unique set of physical properties [8-43], including unexpected combination of metallic and

ceramic properties. These properties that can be attributed to the mostly metallic, with covalent and ionic contributions, of the very strong M-X bond, together with M-A bonds that are relatively weak, especially in shear. The most outstanding and characteristic property that is derived from their layered nature is the ease by which they can be machined.

In the very complete and broad review, Barsoum [5] summarized the physical and structural properties of the MAX phases as follows.

- Being readily machinable, some of MAX phases (e.g. Ti_3SiC_2, Ti_3AlC_2 and Ti_4AlN_3) are elastically quite stiff (at 320 GPa the stiffness of Ti_3SiC_2 is almost 3 times that of Ti metal, with the same density of ~ 4.5 g/cm^3) [9-11]. This implies that some of the MAX phases have the highest specific stiffness values for readily machinable solids – with the exception of Be. In general, it has been predicted, that nanoscale solids, especially laminates, should exhibit unusual and exceptional mechanical properties, which is clearly the case here. With Vickers hardness values in the 2-5 GPa range, these compounds are relatively soft compared to other early transition metal carbides and nitrides.
- They are lightweight and stiff, yet machinable and somewhat ductile at room temperature.
- They are all remarkably damage tolerant [9, 10,11,13].
- They also possess electrical and thermal conductivities in the range of 2-15 x 10^6 $\Omega^{-1}m^{-1}$ and 20-50 W/m K, respectively [3,5,9,26,27,32-34].
- One of the most interesting and fascinating properties of the MAX phases has to be their mechanical response: deformation of Ti_3SiC_2 under compression is quasi-

plastic (inelastic) and yet fully reversible even at 1 GPa at room temperature [37]. This implies that at least Ti_3SiC_2, and possibly all others MAX phase materials, do not work harden at room temperature.

- The basal planes of Ti_3SiC_2 exhibits a coefficient of friction ($\approx 2 \times 10^{-3}$), which is comparable to the lowest values measured for the best solid lubricants (e.g. MoS_2 and graphite) [19]. Even after 6 months' exposure to air, the friction coefficients remained below 5×10^{-3} indicating that these basal planes are chemically robust and most probably also wear resistant.

Most of the work to date [9-11, 12-15, 18-20] has been done on Ti_3SiC_2. Important features of the behavior of Ti_3SiC_2 established thus far include machinability similar to that of graphite [9-11], damage tolerance [13] and good oxidation resistance [14]. Ti_3SiC_2 has a relatively low density, non-susceptibility to thermal shock [10], a brittle to a pseudo-ductile transition at 1200°C, with respectable yield points at 1300°C (100 and 500 MPa in flexure and compression, respectively) together with a more than 50% strain at failure [15]. Each of these properties makes Ti_3SiC_2 a viable candidate for numerous applications.

A. Mechanical Response (Fracture Properties)

As emphasized in Ref 5, the mechanical properties of the MAX phases can be traced to the following 3 facts: (A) Basal slip, and only basal slip, is operative at all temperatures. The Burgers vector in the basal plane is 1.5 Å; any nonbasal dislocation would have to have a Burgers vector > 13 Å. Hence the 5 independent slip systems required for ductility are lacking. However, because they posses more operative slip systems than ceramics, they are more damage tolerant, thermal shock

resistant and softer. If the grains are oriented and large, Ti_3SiC_2 is ductile even at room temperature. (B) Because of their high c/a ratios, twinning is unlikely, and has never been observed. Instead, deformation occurs by a combination of glide and the formation of kink bands within individual grains. (C) Because they are confined to the basal planes, the dislocations arrange themselves either in arrays (pileups) on the same slip plane, or in walls (low or high angle grain boundaries) normal to the arrays. Dislocation interactions, other than orthogonal, are difficult and unlikely to occur. Hence dislocations can move back and forth reversibly and extensively resulting in a new physical phenomenon in crystalline solids best described as fully reversible pseudo-plasticity [24].

As expected, due to their nanolaminated nature, the MAX phases are mechanically (in respect to their fracture properties) strongly anisotropic, yet, somewhat surprisingly thermally they are quite isotropic, in contrast to typical layered materials [18]. The bulk dilatometric thermal expansions of the MAX phases fall in the narrow range of 8 to 10 x 10^{-6} K^{-1} [6,9,18]. The thermal expansion anisotropies of these ternaries are much less pronounced than the anisotropy in mechanical properties would suggest.

In the case of Ti_3SiC_2, along the c-axis, the C-Ti-C, C-Ti-Si and Ti-Si-Ti, bonds expand at 5.5, 8.8 and 13 x 10^{-6} K^{-1}, respectively [18]. In other words, along the c-axis, the C-Ti-C bonds are stronger than, and the Ti-Si-Ti bond are weaker than the average Ti-C bonds in $TiC_{0.97}$[18] It is this averaging in bond strengths that explains both the mild anisotropy in thermal expansion and the good agreement between the normalized molar heat capacity values of Ti_3SiC_2 and $TiC_{0.97}$.

Mechanically, however, Ti_3SiC_2 bears little resemblance to $TiC_{0.97}$. The latter is a hard, brittle solid, susceptible to thermal shock; the former is a relatively soft, readily machinable, damage tolerant solid that is not susceptible to thermal shock [44]. Furthermore, since the earliest work on Ti_3SiC_2 the pronounced anisotropy in its mechanical (i.e. fracture) properties has been well documented. For example, the hardness values normal to the basal planes are about 4 times that parallel to them [21,45]. The unusual mechanical behavior of Ti_3SiC_2 can be directly traced to the relative weakness, particularly in shear, of the Ti-Si bonds, the evidence for which is multifold. Thus, Raman spectroscopy [22] reveals the presence of a soft (151 cm^{-1}) phonon shear mode between the Ti and Si planes. These modes that arise from the shear of the $M_{n+1}X_n$ sheets relative to the A-planes are not found in the binary transition carbides and nitrides. In order to truly understand the relationship between bonding and mechanical properties, the anisotropies in the latter have to be studied by carrying out measurements on single crystals. This work must be performed on a clean single-phase specimen are available.

B. Elastic properties:

The most important role of the elastic properties and their temperature dependence is that with their knowledge one could identify correlations between fundamental solid-state phenomena such as lattice vibrations, theoretical strength, free energy, specific heat and thermal expansivity. We believe that the elastic constants and associated physical parameters (i.e., the Debye temperature) will allow a deeper understanding of the relationship between the mechanical properties and the

electronic and phonon structure of these materials. It is well known that elastic properties also can be predicted from *ab initio* calculations.

The elastic properties of Ti_3SiC_2 were first measured by Pampuch *et al* [16,17], who reported Young's, E_{RT} , and shear, μ_{RT}, moduli at room temperature for two different samples. For these samples, hot pressed at 1400 °C for two hours, E_{RT}, and μ_{RT} were 326±11 and 135±4 GPa, respectively. The corresponding values for samples that were sintered at 1600 °C for 2 hours were 286±2 and 120±1 GPa. Poisson's ratio, ν, was 0.193. The samples measured, however, were not single phase, but contained ≈ 10-20 vol. % TiC [17].

Barsoum and El-Raghy [9] in the preliminary work on a single-phase pure Ti_3SiC_2 material, reported room temperature Young's modulus is about 320 ± 10 GPa. Apart from this information no other references were found in the literature on the elastic properties or their temperature dependence for other $M_{n+1}AX_n$ (n>2) phases.

In this work we report what we believe is the first measurements of the temperature dependence of the MAX phases elastic modduli. We present the measurement of E(T), μ(T) and bulk moduli as a function of temperature for Ti_3SiC_2 [1,2] ,Ti_3AlC_2 [2] and Ti_4AlN_3 [2]. Note that the full set of elastic modulii measured on polycrystalline samples were calculated based on an isotropic media approximation. It should also be noted that isotropy of elastic properties alluded to above based on thermal expansion results and this is somehow in agreement with the recent theoretical prediction obtained by Holm *et al* [39] concerning the relative

isotropy of the elastic properties. We will compare these results with our experimental data in the next Ch. 2.

Information about the elastic constants allows one to calculate the Debye temperature, which characterizes crystalline solids perhaps better than any other single parameter. It normally approximates the specific heat Debye temperature at T=0K. In principle, using elastically measured Debye temperature, θ_D, the lattice contribution to the low temperature heat capacity c_p = const x $(T/\theta_D)^3$ can be estimated.

C. Transport Properties:

I will now move from the overview of mechanical properties and begin a discussion of the transport properties (i.e. electronic and thermal properties).

As was mentioned above, most of MAX phases are excellent conductors of electricity and heat; the thermal and electrical conductivities of Ti_3SiC_2 are more than double those of Ti metal. With one possible exception, Ti_4AlN_3, MAX-phase compounds exhibit metal-like temperature dependence of resistivity ρ(T), i.e ρ increases linear with increasing temperature, at least for T>100K [5]. The resistivities of Ti-based compounds are lower than those of Ti and TiCx , the only exception is possibly Ti_4AlN_3 .

As was shown in [31], the Seebeck coefficient of Ti_3SiC_2 is nearly negligible over the 300–800 K temperature range. This led Barsoum *et al* [31] to the conclusion that Ti_3SiC_2 is most probably a compensated conductor, i.e. the current is carried nearly equally by electrons and holes.

To claim to understand electric transport in a solid it is imperative that the density (*n* or *p*) and mobility of the charge carriers be known. For a simple solid with a single carrier, the combination of Hall coefficient R_H and resistivity measurements is usually sufficient. Once determined these parameters can, in principle, be used to explain thermopower and magnetoresistance measurements.

A first attempt to estimate the concentration of the charges carriers in Ti_3AlC_2, Ti_3SiC_2, and Ti_4AlN_3 was made in [32]. Most of results concerning the charge carriers determination in this original work have been shown lately to be incorrect because of the erroneous determination of the Hall coefficient. Recently, we actually re-measured the Hall effect and recalculated these values [3]. The results of this work are reported in Chapters 3 and 4 and Refs 3 and 4..

The resistivity vs. temperature $\rho(T)$ data were measured for some other MAX phases fabricated so far [5,42,43]. Most of these results cover only high temperature range $T > 77K$. Apart from these results, as far as we are aware, the only low temperature work was done recently by the author in collaboration with the Rowan group [3,4]. However, it is well known that from the low temperature $\rho(T)$ fitting using Block-Gruneisen formula $\rho \sim T^5$ one can estimate the characteristic temperature which is close to the Debye temperature obtained from the heat capacity and elastic measurements. This is important information that is crucial in substantiating the validity of the models and myriad experimental results.

The results of the completed electrical transport, magnetoresistance and Hall measurements for Ti_3AlC_2, Ti_3SiC_2, and Ti_4AlN_3 samples are discussed in Chapter 3 and 4. As it will be shown in these chapters, the Debye temperature of these phases

estimated in this way agree well with the values obtained from low temperature specific heat and elastic measurements.

Because some of the ternary phases are compensated conductors, in order to determine electron density, n, and hole density, p, as well as their mobilities, extra measurements were required. In the absence of such measurements, we assumed $n = p$, which allowed consistent fitting the resitivity, the Hall coefficient and the magnetoresistance results for Ti_3AlC_2 and Ti_3SiC_2. Surprisingly, the Seebeck coefficient in these compounds remains hole-like at all temperatures [43]. Similarly, Ti_4AlN_3 is a p-type conductor at room temperature. As mentioned above, Ti_3SiC_2 is unique; its Seebeck coefficient is negligible over at least 800 K; no other solid behaves this way. The full implication of this result is that Ti_3SiC_2 is a compensated conductor; it conducts electricity by holes and electrons with nearly identical concentrations, i.e. $n = p$.

Thermal transport (thermal conductivity, thermoelectric power, i.e. Seebeck coefficient, and heat capacity) measurements are very important because they can in principle, but not easily be used for checking the validity of the theoretical models.

From the band structure calculations [38,39] one can evaluate the bulk moduli, elastic constants and Debye temperature. To measure the density of states at the Fermi level low temperature heat capacity can be used. These measurements also quantify the Debye temperature. The density of states near the Fermi level for Ti_3SiC_2 were measured twice and hover around 5 (ev.unit cell) [18,39], in excellent agreement with theoretical values [40-42]. The agreement between the values for Ti_4AlN_3 is not as good, most probably is related to non-stoichiometry. In spite of

quite intricate interplay of structure and transport properties in these compounds, their thermal properties can be traced form the strong contribution of the phonon scattering on defects present in the less stoichiometric Ti_4AlN_3.

It was established earlier [5,9] that for the most part the MAX phases are excellent heat conductors because they are excellent electrical conductors. With the exception of some Al-containing MAX phases, the phonon contribution to the total thermal conductivity is small, particularly at high temperature where the results are relatively simple to understand. Given the high elastic constants of these phases, this is a somewhat surprising result. A partial answer to the question – based on a limited set of compounds - has recently been proposed [5,18]; namely that the A-group element acts as a rattler in the MAX structure. Such rattlers have been shown to be potent phonon scatterers. The best phonon conductors to date have been the Al-containing ternaries. One possible reason for this state of affairs is that the Al atoms are better bound to the structure than other A-group elements in general.

Due to MAX-phase materials potential applications they have been extensively studied at elevated temperatures. Very few results have been published on the low-temperature properties of these materials. It should be noted that the knowledge of the low-temperature properties can help to reveal the nature of the fundamental physical characteristics, such as elastic moduli, electrical and thermal conductivities, thermopower and heat capacity.

1.3 Objectives and Scope of Work

The intent of this work is to create substantial experimental database of the low temperature physical properties of the MAX phases to obtain a basic understanding of the physics of these materials. This will be achieved by performing a systematic characterization of their fundamental elastic, electronic, magnetic and thermal properties as function of temperature and composition.

The objectives of this work include:

- Measure Young's and shear moduli of MAX materials as a function of temperature using ultrasonic technique from cryogenic to room temperature.
- Using this experimental data calculate fundamental parameters describing these materials (i.e. Debye temperature).
- Analyze existing theoretical calculation of the elastic properties and compare them with the experimental results to select a correct model
- Measure the electronic and galvanomagnetic properties of the MAX phases over a wide range of temperatures and magnetic fields.
- From this data analyze and predict the type, density and mobilities of the charge carriers using band theory and correlate with the density of states calculations.
- Identify the composition effect on the physical properties of the isostructural compounds by investigating them at low temperatures.
- Study the effect of alloying on M, A or C sites by measuring resistivity and galvanomagnetic properties of substituted materials. Predict the effect of this alloying and its influence on the conduction mechanism. It is our intention to

determine conduction mechanisms for as many materials in the MAX-phase family as possible.

The results obtained from these measurements and substantial interpretations are presented in this thesis.

2. Low Temperature Dependence of the Elastic Properties of Ti_3SiC_2 Ti_4AlN_3, and $Ti_3Al_1C_2$

2.1 Introduction

This chapter contains the first data on the elastic properties temperature dependence of the $M_{n+1}AX_n$ with n=2. Here we present the combination of the results published in two papers [1,2] concerning the Young's and shear moduli measured ultrasonically in 50-300K temperature range for Ti_3SiC_2, Ti_4AlN_3, and $Ti_3Al_{1.1}C_{1.8}$. In the original paper, the chemistry of the latter was assumed to be $Ti_3Al_{1.1}C_{1.8}$. Since that time, the actual composition was measured and found to be Ti_3AlC_2; the latter will be used here.

As it was mentioned in Introduction, the only data on Young's modulus of the single phase Ti_3SiC_2 sample were obtained at room temperature in [9]. The modulus was deduced from the slope of the stress-strain curve.

In our earlier work [1] we reported the first nondestructive measurements of Ti_3SiC_2 elastic moduli as a function of temperature. The elastic moduli were determined from ultrasonic (shear, *Vs,* and longitudinal, V_L) velocities measurements using the following equations [47]:

$$E = V_s^2 \, \rho \frac{(3V_L^2 - 4V_s^2)}{(V_L^2 - V_s^2)} \tag{1}$$

$$\mu = V_s^2 \rho \tag{2}$$

$$\nu = \frac{E}{2\mu} - 1 \quad (3)$$

where E and μ and ν, are, respectively, the Young's and shear moduli and Poisson's ratio. Specimen density, ρ, was measured using Archimedes' principle. In Ref. 1 ρ was 4.47gm/cm^3. The observed density of these samples was about 0.7% less than the theoretical one indicating the presence of some porosity and voids. The concentration of TiC in the sample was less than 1 vol. %. From [1], based on measured velocities room temperature E_{RT} and μ_{RT} were, respectively, 322 ± 2 and 133.6± 0.8 GPa. Poisson's ratio was 0.2 (± 0.007). Interestingly, these values were in excellent agreement with previously reported values [9,16] (see Table 1).

In that paper we estimated the Debye temperature using an expression equivalent to [47]:

$$\theta_D = \left(\frac{h}{k}\right)\left(\frac{3\,n\,\rho N_{Av}}{4\,\pi\,m}\right)^{1/3} v_m \quad (4)$$

where:

h - Plank's constant

k - Boltzmann's constant

ρ - density

n - number of atoms per molecule

N_{Av} – Avogadro's number

m – molecular weight

V_m - mean sound velocity defined as [43] by averaging shear V_s and longitudinal V_L sound velocities:

$$V_m = [\frac{1}{3}(\frac{1}{V_L^3} + \frac{2}{V_s^3})]^{-1/3} \quad (5)$$

In our early work [1], using the measured room temperature value of V_m for Ti_3SiC_2 , θ_D was erroneously calculated to be 427 K, because the molecular weight, rather than the mean atomic weight, was used. The correct Debye temperature is 784 K [2], which is roughly 8 % higher than most recent determination of the Debye temperature from low temperature heat capacity measurements , viz. 715 K [35].

In the later work [2] we re-measured the temperature dependence of the elastic constants of Ti_3SiC_2 and the related ternaries Ti_3AlC_2 and Ti_4AlN_3 in the 50-300 K range. In addition we measured the elastic properties of Ti_3SiC_2 as a function of grain size. The intent was to check the assumption that above ≈ 150 K the moduli of these materials should, like most all other materials, decrease linearly with increasing temperature. This is expected since no phase transitions occur in this material up to at least 1600 °C [18].

2.2 Experimental Details

The processing details have been presented elsewhere [9]. In Ti_3SiC_2 samples used in work [1] the microstructure of the sintered material consisted of equiaxed fine grains ≈ 3-5 μm in diameter. The concentration of TiC in the sample was less than 1 vol. %. The specimen was machined into a 9 x 10 x 18 mm^3 parallelepiped sample. Specimen density was measured hydrostatically with experimental uncertainty of 0.1%. The observed density of these samples from the work [1] was about 0.7% less of the theoretical one indicating the presence of some porosity and voids.

The fabrication procedure details for the $Ti_3Al_{1.1}C_{1.8}$, Ti_4AlN_3 and Ti_3SiC_2 samples can be found in [26], [27,34] and [28], respectively. In brief, Ti_3SiC_2 polycrystalline samples were fabricated by reactive hot isostatic pressing (HIP) of TiH_2, SiC and graphite powders at 1600°C for 4 hours under a pressure of 40 MPa. Titanium hydride (Timet, Henderson, NV, d_m = 12 μm), SiC (99.7 %, d_m = 4 μm, Atlantic Equipment Engineers, Bergenfield , NJ), and C powders (99%, d_m = 1 μm, Aldrich, Milwaukee, WI) were weighed and dry mixed in a V-blender for 2 hours to yield the 3:1:2 stoichiometry. Prior to HIP the compacts were heated in vacuum to dehydride the Ti. All samples in this set of measurements were fully dense. For Ti_3SiC_2, another two microstructures were examined; a fine (5-10 μm) grained structure and a coarse (20-200 μm) grained one [28]. The dimensions of the fine and coarse-grained Ti_3SiC_2 samples were, respectively, 9 x 10 x 15 mm^3 and 8.8 x 10 x 13 mm^3. The samples contained < 2 vol. % TiC and SiC. The Ti_4AlN_3 samples were 10 x

12 x 24 mm^3 in size, and contained ≈ 1-3 vol. % TiN. The $Ti_3Al_{1.1}C_{1.8}$ sample was 10 x 10 x 27 mm^3 and contained ≈ 4 vol. % Al_2O_3 as a secondary phase.

The elastic constants and their temperature dependencies were measured in the 50-300 K temperature range using a standard ulstrasonic pulse-echo method utilizing the heterodyne phase detection technique (PST) described in detail elsewhere [1, 46]. One can find more details on experimental techniques for elastic constant measurements in Appendix C. The set-up used in this work was described elsewhere in detail [46]. This apparatus measures the change in the time of flight by decomposing each individual echo into a quadrature and in-phase component and is capable of resolving relative changes in sound velocity with precision up to 10^{-5}. The PST also measures the absolute sound velocity in the material with an accuracy of about 0.5%. The relative changes in transit times were recorded for each temperature point and the absolute velocities were calculated at 300 K and 20 K. The temperature was controlled by a LakeShore temperature controller. To check the validity of the data calculated from the PST, the sound velocity was also calculated by digitizing and storing each echo pattern. Fast Fourier Transform, FFT, of these patterns was then used to deduce the time of flight. The velocity determined from the FFT was within 0.3 % of the values measured by the PST method. Two Li-niobate transducers (X –cut is for excitation longitudinal wave, and Y-cut is for a shear waves) tuned to the resonant frequency of 15 MHz was used for all these measurements. A photograph of the sample holder and installed specimen with the transducer mounted on the facet is shown in Fig 1. The transducers were bonded to the samples with the different bonding agents to provide adequate coupling of the

acoustic waves over a wide temperature range. For the room temperature measurements, phenyl salicilate (Salol, Merck, Inc.) was used for both transverse and longitudinal waves. In the intermediate temperature range the transducers coupled to the sample with a thin layer of Nonaq Cork grease (Dow Corning). At the lowest temperatures, silicone (GE Caulking compound) was used. The gaps in the data represent regions where the coupling was deemed inadequate.

2.3 Results and Discussion

The experimental results on measured ultrasonic velocities in Ti_3SiC_2 at room temperature along with the calculated modulii are summarized in Table 1 (taken from the early work [1]).

The temperature dependencies of the moduli for Ti_3SiC_2 are plotted in Fig. 2. A least square fit of the results yields:

$$\frac{E}{E_{RT}} = 1 - 0.95 \times 10^{-4} (T - 298) \qquad T > 130 \text{ K}$$

$$\frac{\mu}{\mu_{RT}} = 1 - 1.43 \times 10^{-4} (T - 298) \qquad T > 130 \text{ K} \qquad (6)$$

There are several differing ways of interpreting the results shown in Fig. 2. Typically the temperature dependence of the shear moduli of metals and simple binary compounds is represented by the following relationship [50]:

$$\mu(T) = \mu_{RT} [1 - K (\frac{T - 300}{T_M})] \quad (7)$$

where T_M and T are, respectively, the melting points and the temperature of interest, both in degrees Kelvins. K is a constant of the order of 0.5. To check the validity of this expression for Ti_3SiC_2 is problematic because Ti_3SiC_2 does not melt congruently, but decomposes (like other M_2AX compounds (e.g. [5]), peritectically at ≈ 2200 ± 20 °C. Based on Eq. 7, a plot of $d(\mu/\mu_{RT})/dT$ versus $1/T_M$ should yield a straight line from which the "equivalent" melting point for Ti_3SiC_2 can be estimated. That such a plot of select elements and compounds yields a straight line is shown in Fig. 3. From the plot, K ~ 0.57 and the r^2 value is > 0.95. Based on the value of $d(\mu/\mu_{RT})/dT$ for Ti_3SiC_2 (-1.43×10^{-4}) and Eq. 8, the equivalent melting point of Ti_3SiC_2 is ≈ 2600 °C. This value is reasonably close to the reported decomposition temperature to be plausible.

The temperature dependencies of the Young's moduli of $Ti_3Al_{1.1}C_{1.8}$, Ti_4AlN_3 and Ti_3SiC_2 (for two grain size samples used in [2]) are plotted in Fig. 4a and summarized in Table 2. The corresponding values for the shear moduli are shown in Fig. 4b. The least squares fit of the results shown in Fig. 4b, yields:

$$\mu/\mu_{RT} = 1 - 1.5 \times 10^{-4} (T - 298) \text{ for } T > 125 \text{ K and}$$

$$\mu/\mu_{RT} = 1 - 1.2 \times 10^{-4} (T - 298) \text{ for } T > 125 \text{ K}$$

for Ti_4AlN_3 and $Ti_3Al_{1.1}C_{1.8}$, respectively. These expressions are only valid for T > 125 K; at lower temperatures the elastic constants tend to plateau out. The temperature dependencies of the Young's moduli of the two compounds are also comparable (Table 2).

There is practically no difference between the Young's and shear moduli or their temperature dependencies of the fine and coarse-grained Ti_3SiC_2 samples (Fig. 4a). For reasons that are not entirely clear, the room temperature Young's and shear moduli obtained in [2] were ≈ 4 % higher than our previous determination [1]. One of the possible reasons of this variation may be related to the presence of some voids in the samples used in [1]. The slopes, $(d\mu/\mu_{RT})/dT$, however, are identical (Table 2). It is also worth noting that the bulk modulus calculated herein, 184 GPa, is in reasonable agreement with recent direct measurements on Ti_3SiC_2, viz. 206 ± 6 GPa [36].

Not surprisingly, given the similarities in structure and properties of these ternary compounds, their moduli are all within 10 % of each other. The temperature dependencies of the shear moduli are also quite comparable and within 20 % of each other. Consistent with these results is the fact that the thermal expansion coefficients of Ti_4AlN_3 [27], $Ti_3Al_{1.1}C_{1.8}$ [26] and Ti_3SiC_2 [18] are, respectively, 9.0 x 10^{-6}, 9.7 x 10^{-6} and 9.2 x 10^{-6} K^{-1}.

It has also been suggested that the temperature dependence of E could be expressed as [51]:

$$E = E_o - \frac{S}{\exp(\frac{T_E}{T}) - 1} \quad (8)$$

where E_o, S and T_E are, respectively, Young's modulus at 0 K, a constant and T_E is related to Einstein's temperature. In case of Ti_3SiC_2 , a best fit of the data (dashed line in Fig. 2b) by Eq. 8 yields E_o = 330.8 GPa, S = 19 GPa and T_E = 510K. From the value of T_E the Debye temperature, θ_D, is estimated to be ≈ (4/3) T_E or 680K according to the approach described in [51]. This value, recalculated recently using more recent data and new fitting technique, seems to agree better with the value obtained from low temperature heat capacity work [29] (i.e. 715K) than results presented earlier in [1]. In general, this agreement gives very strong credence of the results. Based on the room temperature value of V_m, calculated value of θ_D is slightly higher than the value (θ_D = 680 K) estimated using the fitting of E(T) curve to Eq. 8.

Based on room temperatures values of v_m, θ_D for $Ti_3Al_{1.1}C_{1.8}$ is calculated to be 758 K, which compares favorably with the value of 764 K measured calorimetrically [35]. Similarly, θ_D for Ti_4AlN_3 is calculated to be 762 K, which, again, is in good agreement with the calorimetric value of 779 K [35]. The corrected Debye temperature for Ti_3SiC_2 (784 K), and the one calculated in this work (780 K), are in excellent agreement with each other and in reasonably good agreement with calorimetric value of 715 K [35]. Both these values are significantly higher than those of Ti ,Ti_3Al or TiN and even comparable to those for C (graphite, viz. 940K) and refractory binary phases such as $TiC_{0.97}$.

As noted in our previous paper [1], the elastic constants and their temperature dependencies measured herein are usually associated with ceramic materials, or very refractory metals such as Mo or W. Hitherto, the price one had to pay for high stiffness, low density solids, has been lack of, or difficulty in machinability. The results of this work make it amply clear that is no longer the case. It should also be mentioned that the shear moduli of these ternaries are weak functions of temperature, implying that these solids should maintain their high stiffnesses to relatively high temperatures. For example, at 1273 K, $Ti_3Al_{1.1}C_{1.8}$, would lose 12 % of its stiffness.

Table I also compares the elastic properties of Ti_3SiC_2 measured in this work to those of $TiC_{0.97,}$ Ti and Mo. It is worth noting that stoichiometric $TiC_{0.97}$ is quite stiff, with Young's and shear moduli of 456-500 [44,45] and 193 GPa [45], respectively. A perusal of the results clearly establishes that:

a) Ti_3SiC_2 is less stiff than $TiC_{0.97}$ but substantially stiffer than Ti. Interestingly, its elastic properties and their temperature dependencies compare quite favorably with those of Mo.

b) The Debye temperature of Ti_3SiC_2 estimated from the elastic measurements is slightly higher than one calculated from heat capacity measurements. This is somewhat quite usual result if one bears in mind the anisotropy of the mechanical response of the MAX phase materials. Given the layered nature of Ti_3SiC_2 and the anisotropy in the strength of its various bonds, one may expect that at least two, not just one, characteristic temperatures (i.e. Debye temperatures) are required to fit the data. This approach is based on representation of the in-plane and out-of-plane (in respect to the layers) vibrational modes associated

with different characteristic temperatures [58]. However, comparative analysis of the available θ_D data for other materials revealed rather small, in general, relative variations in the values of θ_D estimated by different methods for other MAX materials. Though it is well acknowledged that the representation for an structurally anisotropic, multi-element materials by one Debye temperature is an oversimplification, recent experimental results gave an indication that, in principle, these results can be reasonably well treated within the framework of the single-parameter Debye model. For such structurally anisotropic solids as MAX phases, the averaging of their vibration modes, in general, led to the quite adequate results for elastic θ_D calculated in assumption of an elastically isotropic medium where the velocities are independent of crystallographic direction.

This is not surprising result, since this averaging is already presented in polycrystalline materials where the anisotropy is averaged out by the randomly oriented grains. Measured on a polycrystalline specimens (representing an isotropic case) values of the elastic constants would be considered then not a bad approximation of the isotropic solids. In some respect, this notion was also supported by the observed isotropy of Ti_3SiC_2 thermal properties.

In addition to that, the results of our experiments were also supported by the recent theoretical work where Holm *et al* [38] concluded that Ti_3SiC_2 material is essentially elastically isotropic, since c_{11} and c_{33}, as well as c_{12} and c_{13}, were close in magnitude. We came across this theoretical paper on Ti_4AlN_3 and Ti_3SiC_2 mechanical properties after this work was already finished. In [38,39] Swedish group from the Uppsala University obtained a set of elastic constants using density

function theory and compared their results with the values reported in [1,2]. Young's, shear and bulk modulus and Debye temperature values for Ti_3SiC_2 were calculated from the knowledge of the elastic constants evaluated using density of states results. It was shown that our experimental results [2] were in a good agreement with *ab initio* calculations. These values appeared to be less than 10% different from our results calculated experimentally indicating a satisfactory correspondence between theory and experiment.

A complete understanding of the mechanical properties of Ti_3SiC_2 is obviously lacking at this time and more work, both theoretical and experimental, is required. Measurements of single crystal elastic constants would be invaluable at this juncture.

2.4 Conclusions and Summary

In this paper we reported on the temperature dependencies of the elastic properties of Ti_4AlN_3, $Ti_3Al_{1.1}C_{1.8}$ and Ti_3SiC_2. The velocities were measured using a phase sensitive pulse-echo ultrasonic technique in the 50–300 K temperature range. In case of Ti_3SiC_2, Young's, shear and Poisson's ratio are, respectively, 336±3GPa, 133.6±0.8 GPa and 0.2. A least square fit of the data yields, $\mu/\mu_{RT} = 1 - 1.42 \times 10^{-4} (T - 298)$ and $E/E_{RT} = 1 - 0.95 \times 10^{-4}(T - 298)$ for temperatures greater than 130 K. At room temperature, Young's, E_{RT}, and shear, μ_{RT}, moduli and Poisson's ratio of Ti_4AlN_3 are 310 ± 2, 127 ± 2 GPa and 0.22, respectively. The corresponding values for Ti_3AlC_2 are 297.5 ± 2 GPa, 124 ± 2 GPa and 0.2. Both

moduli increase slowly with decreasing temperature and plateau out at temperatures below ≈ 125 K. A least squares fit of the temperature dependencies of the shear and Young's moduli of Ti_4AlN_3 yield: $\mu/\mu_{RT} = 1 - 1.5 \times 10^{-4} (T - 298)$ and $E/E_{RT} = 1 - 0.74 \times 10^{-4} (T - 298)$, for T >125 K. The corresponding relationships for $Ti_3Al_{1.1}C_{1.8}$ are: $\mu/\mu_{RT} = 1 - 1.2 \times 10^{-4} (T - 298)$, and $E/E_{RT} = 1 - 0.84 \times 10^{-4} (T - 298)$ for T >125 K.

The Debye temperature of these materials was calculated using averaged sound velocity. The elastic Debye temperatures calculated for Ti_4AlN_3 and Ti_3AlC_2, as well as Ti_3SiC_2, are all above 700 K, in agreement with values calculated from low temperature heat capacity measurements. This result is also in a good agreement with the value predicted from the fitting of E(T) curve.

3. Magnetotransport Properties of the Ternary Carbide Ti_3SiC_2 in the 4-300K Temperature Range [1]

3.1 Introduction

To date the most studied of MAX phases materials is Ti_3SiC_2. Its physical properties have been extensively characterized since it was successfully synthesized as a fully dense, single-phase bulk material at Drexel University in 1996. It is anomalously soft for a transition metal carbide (Vickers hardness values from 2-4 GPa) and readily machinable with a manual hack saw, regular high speed tool steels with no lubrication or cooling required. Ti_3SiC_2, is elastically stiff (Young's moduli > 300 GPa) [5,9,10], damage and thermal shock tolerant and behaves quasi-plastically under compression [21].

In the last few years several band structure calculations of Ti_3SiC_2 have been performed [38-42]. Two of those papers [40,41] predict a density of states at the Fermi level $N(E_F)$ of about 5 states/eV unit cell. These values are in excellent agreement with the values calculated from low temperature heat capacity measurements [29]. The Debye temperature of Ti_3SiC_2 is also quite high and ranges from 715 to 780 K depending on the method of measurement [2,29].

It is a good thermal and electrical conductor. The room-temperature electrical conductivity is 4.5×10^6 $(\Omega m)^{-1}$, roughly twice that of pure Ti, and more than 4

[1] This chapter is reproduced practically without changes as it appeared in Phys Rev B [3]
Acknowledgements: The authors thank Dr. S. Tyagi for helpful discussions and suggestions. We also acknowledge useful discussions with Dr. V. B. Krasovitsky. This work was partially funded by the Division of Materials Research of the National Science Foundation (DMR, 0072067). The support of the Humboldt and Max Planck Foundations to one of the authors (MB) during his sabbatical leave in Germany is also gratefully acknowledged.

times that of near stoichiometric TiC [9,31,32]. Recently Yoo *et al*. have shown that the thermoelectric power of Ti_3SiC_2 is negligible at least over the 300-850 K temperature range [31]. This fact led Barsoum *et al.* to the conclusion that Ti_3SiC_2 is a compensated conductor [32], in which the concentration of electrons, n, was equal to the concentration of holes, p. In addition, to account for the fact that the Hall coefficient fluctuated around zero, the mobilities of the holes and electrons were also assumed to be equal. As this work shows the Hall coefficient is not zero. Part of the problem in the previous work can be traced to the fact the latter were performed in relatively low (0.8 T) magnetic fields causing the Hall voltage to be around the noise level of the measurements.

In this work, we characterize the electronic transport in Ti_3SiC_2 by performing electrical conductivity, Hall constant and magnetization measurements over the 4 to 300K temperature range and magnetic fields up to 5T. In what follows, we discuss the electronic properties of Ti_3SiC_2 derived from these new experimental results. New insight is obtained on the electronic conduction mechanism in Ti_3SiC_2 in light of the two-band model.

3.2 Experimental Methods

Three samples (two six-probe Hall bars and one parallelepiped shaped specimen) of various thicknesses (0.2 – 1.3 mm) were cut from Ti_3SiC_2 sample with extra large (1 to 2 mm) grains phase fabricated using the following sequence: reactive sintering, hot forging, and a 1600 °C anneal for 24 hrs. The forging oriented

the grains and the annealing allowed them to grow to millimeter sizes. The fabrication details and microstructure are described elsewhere [24]. Despite the fact that the grains were quite large, the samples are to be considered polycrystalline, albeit with few grain boundaries.

The Hall voltage and magnetoresistance, MR, were measured sequentially using pairs of the six leads in a gas flow cryostat over the 4.2 – 300K temperature range and at magnetic fields, *B*, up to 5T. Current contacts were applied with either silver epoxy or Wood's metal. Voltage probes were attached using silver epoxy and annealed gold wire. The voltage sensitivity was roughly 100nV. No contact heating was observed for currents up to 300mA. The temperature was monitored and controlled using a Lake Shore temperature controller and cernox temperature probe which was affixed to the sample holder. The small magnetoresistive component of the Hall voltage was eliminated by magnetic field reversal and subtracting the measured voltage. Thermal emf's were eliminated using a current reversal technique. The magnetic susceptibility measurements were done with a Physical Property Measurement System (Quantum Design).

3.3 Results and Discussion

The temperature dependence of the resistivity $\rho(T)$ for two different samples is shown in Fig. 5. For one sample the measurement was over the entire temperature range; for the second sample the residual resistivity in the low T region was studied in detail. A departure from the typical metal-like linear resistivity region is observed

at temperatures below 90 K. The experimental data was approximated by a Bloch formula using a T^5 law in the low temperature region (insert, Fig. 5). The Debye temperature Θ_D obtained from this fitting yields Θ_D = 830K, which is in good agreement with the value of 760K determined from elastic measurements [2], but higher than those measured from low temperature heat capacity [29]. The experimental results along with the published data are summarized in Table 3, and in general the agreement between the various measurements of ρ(300) and dρ/dT is excellent. Figure 6 shows the Hall voltage as a function of the magnetic field for several temperatures. In the 4 to 200 K temperature range, the Hall voltage is a linear function of magnetic field up to 5T. From these results the Hall coefficients, R_H, were calculated at different temperatures and found to have a weak temperature dependence above 100K, but a stronger dependence at lower temperatures (in the small angle electron-phonon scattering region - see Fig. 2b). In the presence of two isotropic bands with different types of carriers (possessing different effective masses or signs), in a weak field limit, the magnetoresistance ρ(H) and Hall effect can be expressed respectively as [54]:

$$\rho(H) = \frac{\rho_1\rho_2(\rho_1+\rho_2) + (\rho_1 R_2^{\,2} + \rho_2 R_1^{\,2})B^2}{(\rho_1+\rho_2)^2 + (R_1+R_2)^2 B^2} \qquad \textbf{(9)}$$

$$R_H = \frac{R_1\rho_2^{\,2} + R_2\rho_1^{\,2} + R_1R_2(R_1+R_2)B^2}{(\rho_1+\rho_2)^2 + (R_1+R_2)^2 B^2} \qquad \textbf{(10)}$$

where R_i and ρ_i are the Hall constant and resistivity of the specific band, respectively. In the presence of a second group of degenerate charge carriers, the MR can be approximated and expressed in terms of mobilities, μ_I, of the each band by:

$$\Delta\rho/\rho \approx \sigma_1\sigma_2(\mu_1 - \mu_2)^2 B^2/(\sigma_1 + \sigma_2)^2 \quad (11)$$

and the σ_i's are the conductivities of each band. In the special case that the concentration of electrons, n, is equal to that of the holes, p, and given that the mobilities of the electrons, μ_n, is negative, while that of the holes, μ_p, is positive, Eq. 11 simplifies to:

$$\Delta\rho/\rho \approx |\mu_n\mu_p| B^2 \quad (12)$$

wherein the MR is proportional to B^2.

Furthermore, in the low field limit, Eq. 10 can be expressed as:

$$R_H = (1/e) (\mu_p^2 p - \mu_n^2 n) / (p \mu_p + n \mu_n)^2 \quad (13)$$

For n = p, it simplifies further to:

$$R_H = (1/ne) \{(1 - b^2)/ (1+ b)^2\} \quad (14)$$

where $b = \mu_n/\mu_p$ – the ratio of mobilities. In this case, R_H will not be a function of B.

The transverse MR is shown in Fig.8. At 4.2 K, the MR is indeed dominated by a positive quadratic field dependence and can be represented to an accuracy of ± 2% by the expression $\Delta\rho/\rho(B) = 2.06 \times 10^{-3} B^2$ (Fig. 8). Furthermore, R_H is field independent (Fig. 6). These results lead us to the conclusion that, in the two-band model framework, Ti_3SiC_2 is most probably a compensated material, i.e. $n \sim p$. The negligible value of thermopower also supports this conjecture [31].

In common Hall experiments the electrical conduction is dominated by a single type of carrier, and the sign of R_H dictates which type of carrier is mainly responsible for the charge transport. It is easy to see from Eq. (14) that R_H is zero at $b^2 = p/n$. In this regime, when the product of concentration by the square of mobility is equal for both types of carriers, the opposite influence of electrons and holes on R_H makes the measurements extremely sensitive to any changes in either carrier densities or mobilities. This may occur due to the crystalline quality, i.e. grain size, impurity, defects, texturing, etc. Special care must thus be taken to check the effect of charge densities and mobilities.

Between Eqs.12-14 and the simple expression for conductivity, there are 3 unknown. Solving the equations simultaneously at 4.2 K along with the fitting of the experimental data $\Delta\rho/\rho$ (B) one obtains: $\mu_p = 3.6 \times 10^{-2}$ m^2 /Vs and $\mu_n = 2.2 \times 10^{-2}$ m^2/Vs , b~ 0.6, and $n = p = 0.6 \times 10^{28}$ m^{-3}. If one further makes the assumption that n, p and b are not functions of temperature, one obtains that at room temperature, $\mu_n \sim 2.3 \times 10^{-3}$ m^2 /Vs and $\mu_p \sim 4 \times 10^{-3}$ m^2 /Vs.

It is interesting to note that these values are in a good agreement with the value of mobility of ~ 4.5 x 10^{-2} m^2/Vs calculated from the approximate expression for MR $\Delta\rho/\rho(B) \sim \kappa (\mu B)^2$ derived for the degenerate dominating charge carriers in case of impurity (ionic) scattering as a dominating mechanism (for low temperatures, 4.2K $\kappa \sim 0.5$ [55]). It should be noted from the theoretical calculations [40,41], that the ratio of the DOS on the Fermi surface of Ti 3d (electrons) to Si 2s (holes) is of the order of 10. This is consistent with our calculations and the fact that the effective masses are large and the electron mobilities are low.

Interestingly the effective carrier density calculated assuming only one type of carriers are present, vis. $R_H = 1/ne$, gives an effective charge carrier density of 1.78 x 10^{28} m^{-3} at room temperature. In fact, it is not unreasonable to assume that the Hall mobility, $\mu_H = R_H\sigma$, can be also used to estimate the mobility of the dominating carrier. Then, at room temperature, $\mu_H \sim 1.6 \times 10^{-3}$ m/Vs, and $\mu_H \sim 3.1 \times 10^{-2}$ m^2/Vs at 4K. These calculations provide the margin of the applicability of the two-band model. This estimate led us to conclude that we are in the low magnetic field limit, since the product $\mu_H H < 2\pi$, and the effect of the open orbits can be considered minimal.

Care must be taken when one calculates the effective charge concentration, since anisotropy and scattering mechanisms were disregarded in Eq. (11). With a more rigorous look at the MR data, one can observe a slight departure from the quadratic behavior at higher fields (a presence of a linear term in the MR vs B^2 fitting . The MR saturation in the strong field may be evidence for deviation from

the compensated regime. However, the actual magnitude of this effect is rather small and can be neglected.

Finally, the magnetic susceptibility was measured at 5 and 300K. The magnetization, M, appeared to be a linear function of the magnetic field, B, and was found to be independent of temperature or B. The measured value of susceptibility is $\chi \sim 4.1 \times 10^{-6}$. The fact that χ measured in this work is temperature-independent suggests that Pauli spin magnetization theory of the conduction electrons may be applicable to derive and evaluate the effective mass. For a free electron gas:

$$\chi = \mu_o \mu^2_B \, N(\varepsilon_F) \qquad (15)$$

where ε_F - Fermi energy , μ_o – permeability of free space and μ_B - Bohr magneton. From the knowledge that nearly all states below ε_F are occupied at low temperatures, one can calculate $N(\varepsilon_F)$ from χ. After accounting for Landau diamagnetism and band effects, Eq. (15) generally agrees within of factor of 2 with the measured susceptibility. From this one finds, $N(\varepsilon_F) \sim$ 1-2 states/eV unit cell, which is in good agreement with heat capacity results, and theoretical calculations [29,40,41]. This is especially true considering the following simplification made to calculate this value: (a) χ contains the diamagnetic component due to the electrons of the atomic core, (b) in fact , the valence electrons are not completely free – the rest mass must be replaced by the effective mass in $N(\varepsilon_F)$, (c) the value of χ can be influenced by electron-electron and electron-ion interactions. The density of states estimated by Eq. 15 translates to a carrier concentration of $\sim 0.5 \ldots 0.9 \times 10^{28}$ m^3 calculated based

on an isotropic spherical band assumption. This result is in excellent agreement with our Hall effect calculations.

3.4 Conclusions

Our experimental results can be explained to some extent by an isotropic two-band model in the weak magnetic field limit. More satisfactory agreement can be achieved by taking into account the topology of the Fermi surface and the effect of the open electron orbits in the case of strong magnetic fields. The Hall effect and transverse MR have been measured as a function of temperature in the 4 to 300K range and magnetic field up to 5 T. From these measurements the mobility and carriers concentration were calculated. The Hall coefficient was found to be almost independent B and T. These, along with the fact that the MR is a quadratic function of H, imply that, as assumed earlier, Ti_3SiC_2 is a compensated conductor with $n \approx p$. More limited data from microstructurally different samples are also generally consistent with our results. We also measured the magnetic susceptibility in a wide range of temperatures and found that magnetic properties of Ti_3SiC_2 are independent of temperature. The charge carriers concentration obtained from the magnetic susceptibility values is in agreement with the Hall effect and MR results. The mobility values of Ti_3SiC_2 are quite comparable to ones for TiC_x, despite the latter having much lower conductivity. That is probably related to the fact, that the charges carrier concentrations are higher in Ti_3SiC_2, while both compounds are quite similar

thermally. Thus, there we are able to present new reliable experimental data that shed more light on the conduction mechanism operative in Ti_3SiC_2

4. Low Temperature Electronic and Transport Properties of Nanolamintes Ti_3AlC_2 and Ti_4AlN_3 [2]

4.1 Introduction

The electrical properties and their relationship to chemistry of the MAX phases are needed to be more completely characterized and understood at low temperatures. This chapter is a continuation of our study of the electrical and transport properties of the 312 and 413 phases, namely, Ti_3AlC_2 and Ti_4AlN_3.

At 0.39 μΩm, the room temperature resistivity of Ti_3AlC_2 [26,32] is higher than that of Ti_3SiC_2 (0.22 μΩm) but roughly an order of magnitude smaller than that of Ti_4AlN_3 [27,32]. More recent work [43] reported a lower room temperature resistivity of 0.285 μΩm, with a residual resistivity of ≈ 0.1 μΩm. The resistance of Ti_4AlN_3 is high partly because of its high residual resistivity, which likely reflects the fact that its actual chemistry is 4:1:2.9 rather than 4:1:3 [33,34].

In a recent paper [3] we noted that both the carrier densities and mobilities in Ti_3AlC_2 and Ti_4AlN_3 were, for reasons that were not clear, roughly an order of magnitude off from the same parameters in Ti_3SiC_2 despite their structural similarities. In this paper we carefully characterize the electronic transport in Ti_3AlC_2 and Ti_4AlN_3 by measuring their electrical conductivity, magnetoresistance,

---

[2] This chapter is based on the paper to be appeared in Phys Rev B July 2003 (in press). This research was partially supported by the Division of Materials Research at NSF (Grant Nos. 0072067 and 0114073), the New Jersey Commission on Higher Education, Rowan University and by an award from the Research Corporation. We would also like to thank Mr. A. Procopio and Dr. N. Tzenov for supplying us with the samples used in this work.

Hall effect, thermopower and magnetic susceptibility in an attempt to better understand their overall electronic behavior and previous observations.

4.2 Experimental Procedure

Polycrystalline bulk samples of Ti_3AlC_2 were fabricated by reactively hot isostatically pressing a mixture of titanium, graphite and Al_4C_3 powders at a pressure of 70 MPa and a temperature of 1400°C for 16 h [26]. The samples were predominantly single phase (containing 4 vol. % Al_2O_3) and fully dense with a grain size of ≈ 25 μm. Two polycrystalline parallelepiped-shaped specimens with dimensions 0.2×2.0×12 and 1.3 × 2.3 × 12 mm^3 were cut from a Ti_3AlC_2 sample. The fabrication of the Ti_4AlN_3 samples is described in detail elsewhere [33,34]. For the transport measurements on Ti_4AlN_3 we used two specimens: one with dimensions 0.5×3.17×12 mm^3, the other (1.0 × 1.52 × 15 mm^3) was cut from the same batch used in [31].

Four- and five-probe measurements were carried out as a function of temperatures, *T,* ranging between 5 and 300 K and magnetic fields, *B,* up to 9 T with a Quantum Design Physical Properties Measurement System (PPMS). The electrical resistivity, ρ, Hall voltage, V_H, and magnetoresistance, (MR = [ρ(*B*)- ρ(0)]/ρ(0)]) were measured using a specially designed sample holder with spring-loaded gold-coated contacts. The voltage sensitivity was roughly 5 nV, and no contact heating was observed for currents up to 300 mA. The MR component of the transverse voltage and extraction of the Hall signal were achieved by either a balancing potentiometer or by magnetic field reversal and subtraction of the measured

voltages. Thermal emf's were eliminated by use of a low-frequency ac current technique. The magnetic susceptibility measurements were carried out on powdered samples; the excitation frequency was varied from 100 Hz to 10 kHz with ac-field amplitude of 800 A/m. The details of the high-temperature Seebeck coefficient measurements can be found in [31] and [32]. The low-temperature Seebeck coefficient was measured with the PPMS.

4.3 Results

The temperature dependence of ρ for Ti_3AlC_2 shows a typical metal-like resistivity; from room temperature to about 80 K the resistivity drops linearly with temperature (Fig. 9). The residual resistivity, ρ_0, of 0.18 μΩm is roughly six times higher than that of Ti_3SiC_2 (0.033 μΩm) [3], indicating the presence of a relatively larger defect concentration in Ti_3AlC_2. The low-temperature data can be reasonably fit with the Bloch formula with the T^5 law, yielding a Debye temperature, $\Theta_D \approx 800$ K, in good agreement with the 760 K determined from elastic measurements [2], but somewhat higher than the value obtained from low-temperature heat capacity measurements [29].

The ρ vs. T curves for Ti_4AlN_3 are essentially parallel to those for Ti_3AlC_2 (and Ti_3SiC_2 for that matter) but are shifted vertically because of the significantly larger residual resistance $\rho_0 = (23.5 \pm 2) \times 10^{-7}$ Ω-m (Fig. 9). Even though ρ_o is relatively large, the fitting of the low-temperature resistivity to the Bloch-Gruneisen formula yields $\Theta_D \approx$ 685 K, which is in reasonable agreement with values of Θ_D =

740 K obtained from elastic [2] and heat capacity measurements [29]. At all temperatures, the Hall voltage, V_H, for Ti_3AlC_2 is a linear function of B up to 9 T (inset Fig. 10a). At the lowest temperatures, the Hall coefficient, R_H, is small but positive; above 100 K it is negative and drops more or less linearly with temperature (Fig. 10a). For Ti_4AlN_3, the dependence of V_H on B is also quite linear and almost independent of temperature (Fig. 10b).

The effect of B on the MR of Ti_3AlC_2 can be well fitted with the expression $MR = \alpha B^2$, where α is a quadratic coefficient equal to 4×10^{-5} m^4/V^2s^2 at 300 K (Fig. 11) and 1.1×10^{-4} m^4/V^2s^2 at 4 K. α drops more or less linearly with increasing temperature (Fig. 12). The MR of Ti_4AlN_3 is small with α no greater than 3×10^{-7} m^4/V^2s^2.

The Seebeck coefficients of both compounds are plotted as a function of temperature in Fig. 13. Also included are the results of previous work [31]. The Seebeck coefficient of Ti_3AlC_2 is positive at all temperatures with a maximum at $\approx$ 700 K. The agreement between the results obtained in this work and previous work [31] is excellent. The response of Ti_4AlN_3 is similar, but the Seebeck coefficient peaks around 300 K and becomes negative at temperatures greater than 800 K. The high-temperature results (solid diamonds) were measured in Korea on the same sample used for the low-temperature measurements (open diamonds) (for details see Ref. [31]). The agreement between the two sets of results is noteworthy. Also included are the results of previous work on a different sample [31]; the agreement with this data is not as good.

4.4 Discussion

Based on the results presented here, and in qualitative agreement with previous work [32], we conclude that for Ti_4AlN_3 - because of the large positive value of R_H, holes are the majority carriers. The behavior is well described by a single-band model in which the dominant carriers are holes with a concentration, $p = 1/(e\ R_H) \approx 0.7 \times 10^{28}$ m^{-3} and mobility, $\mu_p = 3.4 \times 10^{-4}$ m^2/Vs at room temperature (Table 4).

The mobility is relatively low, as expected, presumably because of the point defects – recall the actual stoichiometry is $Ti_4AlN_{2.9}$. It is fairly well established that point defects in binary transition metal carbides in general, and TiC in particular, are potent scatterers of electrons [52]. The low mobility is consistent with the fact that α for this material is small ($\sim 10^{-7}$ m^4/V^{2}s^2). It is interesting to note that the mobilities calculated from the approximate formula, MR ~ $(\mu B)^2$, result in values ($\approx 3 \times 10^{-4}$ m^2/Vs) that agree quite well with those estimated from the Hall effect measurements. Another characteristic of Ti_4AlN_3, noted earlier [32], and confirmed in this work is that the variation from sample to sample tends to be high (Fig. 9). Here again the exact reason for these variations is unknown but most probably reflect variations in chemistry or stoichiometry. Similar arguments can be made to explain the scatter in the Seebeck coefficient results (Fig. 13). Note that the slopes of the lines in Fig. 9 are comparable indicating that the electron-phonon scattering mechanisms in these compounds are comparable.

The situation for Ti_3AlC_2 is more complex. The sign change of R_H (Fig. 10) indicates that a single-band model cannot be used. Since MR is quadratic with, and

V_H is linear in, B the two-band model can be used where the following applies [54,55,57,58,]:

$$\text{MR} = \frac{\mu_n \mu_p np(\mu_n - \mu_p)^2 B^2}{(\mu_n n + \mu_p p)^2} = \alpha B^2 \quad (16)$$

$$R_H = \frac{(\mu_p^2 p - \mu_n^2 n)}{e(\mu_p p + \mu_n n)^2} \quad (17)$$

where μ_n and n represent the mobilities and carrier densities of the electrons. In addition, conductivity, σ, is given by

$$\sigma = \frac{1}{\rho} = e(n\mu_n + p\mu_p) \quad (18)$$

To solve for μ_n, μ_p, n and p one needs an extra constraint. Here we assumed that $\mu_n > \mu_p$ and a range of b values (where $b = \mu_p/\mu_n$) that varied between 0.4 and 0.8 – a range previously shown to be valid for Ti_3SiC_2 [3]. To simplify the math we started at 100 K, where $R_H = 0$ and $\mu_p^2 p = \mu_n^2 n$.

The results for the various values of b are listed in Table II; the following points are salient. The values of n are only weakly dependent on the values of b and/or temperature; they fall in the narrow range of 0.16 to 0.17×10^{28} m^{-3}. At the lower b values, the range of p is a stronger function of temperature. However, since the magnetic susceptibility results are a weak function of temperature (Fig. 14), suggesting a temperature-independent total charge carrier concentration, we sought values of b that led to the smallest variations in p. With this in mind, we conclude

that the more accurate values for n, p, μ_n and μ_p are the ones for which $b > 0.6$, which are listed in Table 5. It is worth noting that when R_H is close to zero, as the case is here, the sign and magnitude of the Hall coefficient are quite sensitive to small variations in the values of the mobilities chosen. For example, if μ_p is changed from 0.0075 to 0.0073 m^2/Vs, R_H changes from $+ 2.2 \times 10^{-11}$ to $- 2 \times 10^{-11}$ m^3/C.

The assumption that n and p remain almost unchanged with temperature is quite reasonable based on the observed metallic nature of the electronic transport in these compounds. As discussed in the preceding paragraph, this conclusion is also supported by the fact that the magnetic susceptibility is relatively temperature independent. Further, it is well established that the conductivity of normal metals at high temperatures depends primarily on the electron-phonon scattering mechanism. Thus, changes in the mobilities should be considered the primary cause of the observed temperature dependencies of R_H and α, rather than changes in n or p. It is thus reasonable to conclude that the negative sign of R_H, at low T, is a direct consequence of the electron mobility being larger than that of the holes. In the case of thermal scattering by acoustic phonons, the mobility normally decreases with increasing temperature as (const) $\times T^{-3/2}$ [55]. The temperature dependence of the reciprocal of the mobility [calculated assuming MR ~ $(\mu B)^2$, plotted in inset in Fig. 12 inset] is consistent with a material for which the dominant scattering mechanism is lattice scattering with a strong contribution due to the presence of neutral impurities (horizontal dashed line) at low temperatures. Examination of this plot and Fig. 10a suggests that the crossover of the dominant charge carrier, from hole-like to electron-like that occurs below 100 K, may be due to this temperature dependent

scattering. The temperature dependence of α representing the square of mobilities also illustrates similar behavior (Fig. 12). It is interesting that a distinct difference in the temperature dependence of the mobility occurs below 100 K, where the impurity effect is more pronounced (residual resistivity region).

The good agreement between the electrical transport parameters calculated here for Ti_3AlC_2 and Ti_4AlN_3, and those for Ti_3SiC_2 and near-stoichiometric TiC_x ($x > 0.95$) measured previously and reported in [41] (Table 4) increases our confidence level in the full set of results. This is particularly true when it is appreciated that the ratios of the density of states at the Fermi level $N(E_F)$ for Ti_4AlN_3 Ti_3SiC_2 and Ti_3AlC_2 - when normalized to a per Ti atom basis (eV-Ti atom)$^{-1}$ - are 0.86:0.83:0.63 [9,29] in good agreement with the narrow range in n and p deduced from our analysis. In retrospect, it is now clear that the R_H results reported in [32] were incorrect; the results obtained here yield a much more consistent and believable set.

Finally it is important to note that the Seebeck coefficients measured for Ti_3AlC_2 and Ti_4AlN_3 (Fig. 13) are in agreement with the parameters listed in Table 4. For both compounds, the Seebeck coefficients are positive since in both cases the majority carriers are holes. It is generally accepted that the temperature gradient driven entropy carriers of the Seebeck measurement scatter differently than the potential energy gradient driven charge carriers of electrical transport. This implies that the entropy carrier mobility will have a different temperature dependence than that of the charge carrier mobility. Here we have a possible method for testing our ideas. If the crossover of the sign of the Hall number is related to a change in total or relative carrier concentration, one would expect to see the signature of the sign

change in the Seebeck voltage. Alternatively, if the sign change is a result of the temperature dependence of the mobilities, the Seebeck may not demonstrate a signature of the change. As seen in Fig.13, the Seebeck coefficient does not change sign, supporting our assumptions above.

4.5 Summary

In this paper we report on the electronic and magneto-transport properties of two Ti-based ternaries; Ti_3AlC_2 and Ti_4AlN_3. In order to determine the effective carrier concentrations and their mobilities, the Hall effect, electrical conductivity, thermoelectric power, magnetic susceptibility and magnetoresistance were measured as a function of temperature between 4 and 300K and at magnetic fields up to 9 T. For Ti_3AlC_2, the Hall voltage is a linear function of magnetic field at all temperatures. At the lowest temperatures, the Hall coefficient is small but positive; above 100 K it is negative and drops more or less linearly with temperature. The magnetoresistance of Ti_3AlC_2 is dominated by a positive quadratic field dependence. The magnetic susceptibility is nearly constant but displays a weak maximum around the temperature where the Hall effect changes sign (≈ 100 K). In contrast, the Seebeck coefficient remains positive up to 800 K, with a maximum at 700 K. The results were analyzed within a two-band framework assuming a temperature-independent charge carrier density and a hole mobility that is slightly smaller than the electron mobility. The model quantitatively accounts for all our observations. The resistivity, magnetoresistance and Hall coefficient of Ti_4AlN_3, on the other

hand, were successfully described within the single-band model, with holes as the dominant charge carriers. This was supported by measurements of the Seebeck coefficient which is positive and peaks at ≈ 300 K. The magnetic susceptibility of Ti_4AlN_3 is also quite temperature independent.

4.6 Conclusions

We completed a systematic set of electronic transport experiments on Ti_3AlC_2 and Ti_4AlN_3. We find that the results for Ti_3AlC_2 can be explained within a two-band model, using a temperature independent number of total charge carriers (although with a higher concentration of holes) and a temperature-dependent ratio of the carrier mobilities. The data for Ti_4AlN_3, on the other hand, were successfully described within the single-band model. To unambiguously determine the exact mobilities of Ti_3AlC_2, one must await the results of further experiments such as thermal transport.

5. Transport Properties of the Solid Solutions $Ti_3Si_xGe_{1-x}C_2$

5.1 Introduction

In order to further understand the physical properties of MAX phases one must investigate other materials. The only way to analyze the role the A-element plays in bonding of these phases is to characterize solid solutions with various concentrations of the A-element, preferably, from the same group. As this chapter shows it is quite instructive to study how the A-element substitutions affect transport properties.

Although to date the most studied is Ti_3SiC_2, two other M_3AX_2 phases also exist with A = Al or Ge. Recently the Drexel group has fabricated fully dense $Ti_3Si_xGe_{1-x}C_2$ phases [55]. The ternary Ti_3AlC_3 has already been studied (see Ch. 4). At this moment very limited information exists about physical properties of the Ti_3GeC_3 and none exist on the properties of $Ti_3Si_xGe_{1-x}C_2$ solid solutions. The purpose of this chapter is report on the electrical conductivities, magnetoresistances, Hall effects, thermopower and the thermal conductivities obtained on fully dense samples of $Ti_3Si_xGe_{1-x}C_2$ with x = 0, 0.25 and 0.5 in the 4 to 300 K temperature range. We also report on the elastic properties at room temperature of the same materials. In future work, we plan to further characterize the electronic transport in the $Ti_3Si_xGe_{1-x}C_2$ phases by measuring their elastic constants , heat capacities and their low temperature dependencies and compare these results with those reported

herein. Our overall goal is to better understand the transport properties of the MAX phases.

5.2 Experimental Methods

For the elastic constant measurements a Ritec RAM 10000 system based on phase sensitive detection technique (PST) was used. This system was quite similar to that described in the Chapter 2 and [46]. This method is able to provide absolute and relative sound velocity measurements with a precision comparable to the method used in [46]. The Young's and shear moduli were calculated by means of ultrasonic echo-pulse time of flight measurements. Ti_3SiC_2 sample was re-measured as a crosscheck. This system is capable to automate signal processing and perform amplitude and phase measurements of pulsed ultrasonic signals at frequencies 5-20 MHz. The system is equipped with a digital data acquisition card for control and measurement functions. Temporal resolutions of 4 ps are possible.

The sample fabrication details are described elsewhere [59]. In general, bulk polycrystalline samples of $Ti_3Si_{0.5}Ge_{0.5}C_2$ and $Ti_3Si_{0.75}Ge_{0.25}C_2$ were fabricated by mixing Ti, C, SiC and Ge powders in order to yield the desired stoichiometry. The mixed powders were then hot isostatically pressed (HIPed). Several bar shaped specimen with dimensions 1 x 1 x 12 mm^3 and 1.5 x 2 x 12 mm^3 were cut for the transport measurements. The samples of $Ti_3Si_{0.5}Ge_{0.5}C_2$ for ultrasonic measurements were 8 x 8 x 8 mm^3 cubes. The Ti_3GeC_2 sample was a cylinder with a 10 mm

diameter and16 mm long. In all cases Salol© was used as the ultrasonic transducer bonding compound.

Hall and resistivity four- and five-probe measurements were carried out as a function of temperatures in 5-300 K range and magnetic fields up to 9 T with a Quantum Design Physical Properties Measurement System (PPMS). The electrical resistivity, ρ, Hall voltage, V_H, and magnetoresistance, (MR = [ρ(B)- ρ(0)]/ρ(0)]) were measured using a specially designed sample holder with spring-loaded gold-coated contacts. The low-temperature thermal conductivity and Seebeck coefficient was also measured with the PPMS.

5. 3 Results and Discussion

Room temperature Young's and shear moduli were calculated from the two independent measurements of the longitudinal and shear sound velocities. Results are summarized in the Table 6. Young's and shear moduli for x = 0.25 and 0.5 phases were slightly lower than that for x = 1 or Ti_3GeC_2. At 714 K, the Debye temperature Θ_D of the latter calculated from the mean ultrasonic velocity (Eq. 4) was about 11% lower than that measured for Ti_3SiC_2 (780K).

It is interesting to compare the effect of composition on the room temperature transport properties. For example, room temperature resistivity (Fig. 15), thermal conductivity (Fig.16) and Seebeck coefficient (Fig.17) remain practically unchanged for all solid solutions as well as for the pure phases. However, the noticeable effect was observable for x = 0.25 and 0.5 at low

temperatures for residual resistivity when defect scattering dominates over the thermal scattering (Fig. 18). The low temperature thermal conductivity peak (see Fig. 16) was also suppressed for the solid solutions. It is also noteworthy that the temperature coefficient of resistivity dρ/dT remains practically unchanged across the entire solid solution range. That value is also the same for Ti_3AlC_2. The slight variation of dρ/dT for x = 0.25 and 0.5 can be interpreted to be due to the contribution of electron-impurity scattering.

Preliminary analysis of magnetoresistance and the Hall effect results utilizing a two-band model, a temperature-independent charge carrier density and a constant relaxation time as a function of the electronic energy, was carried out in the same manner as was done for the isostructural Ti_3SiC_2 (see Chapter 3, [3]) and Ti_3AlC_2 (Chapter 4, [4]) Here again we assume n ~ p. The calculated charge carriers mobilities and concentrations are summarized in the Table 6. As can be seen from this table, the agreement between all phases is more than satisfactory. The carrier concentration results (see Table 7) suggest that the electronic properties vary little between the Ti_3AC_2 phases. These results also clearly indicate that the major effect the solid solution has is on the carrier mobilities, probably as result of diminished scattering length.

5.4 Conclusions

Based on the results presented in this chapter it appears that the A-group element has an effect of the elastic properties of M_3AX_2 solids. And while the carrier

concentrations are quite insensitive to the nature of the A-group element in the M_3AX_2 phases, solid solution scattering results in reduced mobilities.

6. Summary and Conclusions

MAX phases are fascinating new compounds, which most of their physical properties are still unknown. For many phases, their properties are probed only within certain compositional and temperature domains (with the exception of only a few compounds being fully characterized). Clearly much more remain to be done.

However, since these materials are extremely new it is necessary to scan all their properties such as elastic, electric, thermal and mechanical properties. It should be stressed once again that there is no available existing database of physical properties of these solids.

In this work, for the first time, a systematic experimental study of the elastic and electronic properties of the MAX phases was carried out in the 4-300 K temperature range. It has been shown that the knowledge of the low temperature properties provides invaluable information about the physics and properties of the MAX phases. As a result of this work, the elastic constants, electrical resistivity, thermal conductivity and galvanomagnetic effects were characterized as a function of temperature. It was found that the Young's, shear and bulk moduli of these compounds (Ti_3SiC_2, Ti_3AlC_2 and Ti_4AlN_3) obtained from the nondestructive ultrasonic velocity measurements increase slowly with decreasing temperature and plateau at low temperatures. Ti_3SiC_2 has stiffness at 300 K with Young's, and shear, moduli of 335 and 139 GPa, respectively; Poisson's ratio is 0.2. The Debye temperatures of these compounds were also calculated using the mean ultrasonic velocity to be 650-780K. These values agreed well with data obtained from low

temperature heat capacity measurements, viz 715-762K (the lowest value is for Ti_3SiC_2, and highest one - for Ti_4AlN_3).

The electronic transport properties were also characterized from the resistivity, magnetoresistance, Hall effect, Seebeck coefficient and magnetic susceptibility measurements carried out in the 4 to 300K range, and magnetic field up to 9 T. All MAX phases exhibit metal-like temperature dependence of the resistivity. Debye temperature values for most of the phases were determined by fitting $\rho(T)$ using a Bloch T^5 formula. The results obtained were in a good agreement with the value determined from elastic measurements. The carrier density of electrons, *n* and electrons, *p*, and their mobilities were calculated utilizing a semi-classical, isotropic 2-band model. It was shown that most of the $M_{n+1}AX_n$ (n=2) phases (Ti_3SiC_2, Ti_3AlC_2, Ti_3GeC_2) are nearly compensated conductors with $n \sim p$. This result also was is in agreement with conclusions based on the fact that the thermopower in these solids is negligible.

Also, as it was shown that Ti_3SiC_2, Ti_4AlN_3, and Ti_3AlC_2 are very weakly paramagnetic solid, with a susceptibility that is a weak function of magnetic field and, most important, temperature indicating that the total charge concentration, $n+p$, is also constant with total charge carriers (electrons and holes) concentration of $\sim 10^{28}$ m^{-3} .

Extensive study of electronic and magneto-transport properties and analysis of the results suggest that the $M_{n+1}AX_n$ (n = 2) phases can be characterized by relatively high charge carrier mobilities.

The results of this work clearly demonstrated that in order to create a complete picture correlating crystal structure, microstructure, and resulting physical properties of the phases, it is important to extend measurements to other materials of this class, namely, solid solution phases of M_3AX_2 and M_2AX phases. This systematic work characterizing the electronic, magnetic and thermal properties of the MAX phases expands the knowledge of these materials.

At the end, author wishes to believe the experimental results of this work would helped to accelerate our understanding of this new class of potentially very technologically important solids.

7. Future Work

Since about six years the group at Drexel University has undertaken a large working plan to synthesize and characterize MAX phases. In addition to all the known phases, these materials exhibit large solid solution capability in which each of the sublattice M, A and X behave independently and it is expected that upon alloying the elements mix on each sublattice separately.

Probably further experimental work can be done to characterize various composition domains. The plan is to perform heat capacity and speed of sound measurements on many of the MAX phase materials with various solid solution compositions allowing the extraction of the elastic moduli and Debye temperatures. The goal of this study will be to find how good is the agreement between the Debye temperature as determined from calorimetric measurements or specific heats and that determined from elastic measurements.

We also plan to measure low temperature transport properties of another groups of ternary carbides and nitrides (Ti_2AlC, Ti_2AlN, V_2AlC, Nb_2AlC, Cr_2AlC and Ti_2GeC), namely 211 phases, in order to study the effect of the solid substitution in the M-site on the physical and electronic properties in these isostructural compounds. In future work we plan to report on their elastic, thermal and electrical properties in the temperature range 4 to 300K.

Another interesting material to be investigated is V_2AlC. We already showed in our preliminary experiment that the Seebeck coefficient at the lowest temperatures is small and negative; increases with increasing temperature, saturates at ≈ 2 μV/K at

85 K and goes through zero again at 160 K before changing sign from negative (electron like) to positive (hole like). The thermal conductivity in the 100 and 300K temperature range is relatively temperature independent. A peak is observed near 75K suggesting the materials is quite clean. This is further supported by the residual resistivity ratio, which is roughly 10. To investigate the sign change of the dominant charge carriers, we also measured the electrical conductivity and Hall effect. Comparisons of these results will be presented.

List of References

1. Finkel P, Barsoum MW, El-Raghy T. Low temperature dependence of elastic properties of Ti_3SiC_2. J. Appl. Phys. 1999;85:7123-29.

2. Finkel P, Barsoum MW, El-Raghy T. Low Temperature Dependencies of the Elastic Properties of Ti_4AlN_3, $Ti_3Al_{1.1}C_{1.8}$ and Ti_3SiC_2 J. Appl. Phys. 1999;85:7123-29.

3. Finkel P, Barsoum MW, J.Hettinger, Lofland S Magnetotransport properties of the ternary carbide Ti_3SiC_2: Hall effect, magnetoresistance, and magnetic susceptibility Phys. Rev. B, 2001;65: 035113

4. Finkel P, Barsoum MW, Hettinger J, Lofland, and Yoo HI Low Temperature Transport Properties of Nanolaminates: Ti_3AlC_2 and Ti_4AlN_3 To appear in Phys. Rev. B, July 2003 (in press)

5. Barsoum MW. The $M_{N+1}AX_N$ phases: A new class of solids: Thermodynamically stable nanolaminates. Prog. Solid State Chem. 2000;28:201-81.

6. W.Jeitschko H Novotny and F Benesovsky Kohlenstoffhaltige terare Verbindungen (H–Phase) Monatsh Chem. 1963;94:672.

7. Jeitschko W, Nowotny H. Die kristallstructur von Ti_3SiC_2 – Ein neuer komplxcarbid-typ", Monatasch fur Chem. 1967;98:329-37.

8. M. A. Pietzka and J. C. Schuster, Summary of Constitution Data of the System Al-C-Ti J. Phase Equilibria, 1994;15 (4):392.

9. Barsoum MW, El-Raghy T. Synthesis and characterization of remarkable ceramic: Ti_3SiC_2. J. Am. Ceram. Soc. 1996;79:1953-56.

10. Barsoum MW, Brodkin D and El-Raghy T, Layered Machinable Ceramics for High Temperature Applications Scrip. Met. et. Mater,1997;36:535.

11. Barsoum MW, El-Raghy T. A progress report on Ti_3SiC_2, Ti_3GeC_2 and H-phases, M_2BX", J. Mater. Synth. Process. 1997;5:197-216.

12. Barsoum MW, Yaroschuck G and Tyagi S Fabrication and Characterization of M_2SnC (M=Ti, Zr, Hf and Nb). Scrip. Mater., 1997;37:1583.

13. El-Raghy T, Zavaliangos A, Barsoum MW, Kalidindi SR. Damage mechanism around hardness indentation in Ti_3SiC_2. J. Am. Ceram. Soc. 1997;80:513-16.

14. Barsoum MW, El-Raghy T and Ogbuji J Electrochem. Soc., Oxidation of Ti3SiC2 in Air 1997;144: 2508.

15. El-Raghy T, Barsoum MW, Zavaliangos A, Kalidindi SR. Processing and mechanical properties of Ti_3SiC_2, Part II: Effect of grain size and deformation on temperature. J. Am. Ceram. Soc. 1999;82: 2855-62.

16. Pampuch R, Lis J, Stobierski L, Tymkiewicz M. Solid combustion synthesis of Ti_3SiC_2, J. Eur. Ceram. Soc.1989;5:283-91.

17. Pampuch R, Lis, J Piekarczyk J, Stobierski L Ti_3SiC_2 –Based Materials Produced by Self-Propagating High-temperature Synthesis (SHS) and Ceramic Processing J. Mater. Synth. Process 1993:1;2:93.

18. Barsoum MW, El-Raghy T, Rawn CJ, Porter W D, Wang H, Payzant E A and Hubbard C R Thermal properties of Ti_3SiC_2 J. Phys. and Chem. of Solids. 1999:60;429.

19. S. Myhra, J. W. B. Summers and E. H. Kisi, Mater. Lett. 1999:39;6.

20. J. C. Ho, H. H. Hamdeh, M. W. Barsoum and T. El-Raghy Low Temperature Heat Capacity of Ti_3SiC_2 J. Appl. Phys. 1999: 85;7970.

21. T. Goto and T. Hirai,., Chemically Vapor Deposited Ti_3SiC_2, Mat. Res. Bull 1987:22; 2295.

22. M. Amer, M. W. Barsoum, T. El-Raghy, I. Wiess, S. LeClair and D. Liptak, J. Raman Spectrum of Ti_3SiC_2 J. of Appl. Phys. 1998:84:5817.

23. Farber L, Barsoum MW, Zavaliangos A, El-Raghy T Dislocations and stacking faults in Ti_3SiC_2. J. Am. Ceram. Soc. 1998:8;1677-81.

24. Barsoum MW, El-Raghy T Room temperature ductile carbides. Metall. Mater. Trans. 1999;30A:363-69.

25. Barsoum M W, Farber L, Levin I, Procopio A, El-Raghy T and Berner A High-resolution transmission electron microscopy of Ti_4AlN_3, or $Ti_3Al_2N_2$ revisited J. Amer. Cer. Soc.,1999:82;2545-2547.

26. N. Tzenov and M. W. Barsoum Synthesis and Characterization of $Ti_3Al_{1.1}C_{1.8}$ J. Amer. Cer. Soc. 2000;83:825-832.

27. Procopio A T, Barsoum MW and El-Raghy T Characterization of Ti_4AlN_3 Met. Mater. Trans. 2000;87:1701.

28. El-Raghy T, Barsoum M W, Zavaliangos A, Kalidindi S R Processing and Mechanical Properties of Ti_3SiC_2: PartI: Reaction Path and Microstructure Evolution. J. Am. Ceram. Soc. 1999;82: 2849-55.

29. Ho J C, Hamdeh H H, Barsoum M. W and El-Raghy T Low temperature heat capacities of Ti_4AlN_3, $Ti_3Al_{1.1}C_{1.8}$ and Ti_3SiC_2 ibid.1999;86:3609.

30. M. W. Barsoum, L.Farber, T.El-Raghy and I.Levin, Dislocations, Kink Bands, and Room-Temperature Plasticity of Ti_3SiC_2 Met. Mat. Trans. 1999; 30A: 1727.

31. H-I. Yoo, M. W. Barsoum and T. El-Raghy, Ti_3SiC_2 Has Negligible Thermopower Nature 2000;407;581.

32. M. W. Barsoum, H.-I. Yoo, I. K. Polushina, V. Yu. Rud', Yu. V. Rud' and T. El-Raghy, Electrical Conductivity, Thermopower and Hall Effect of Ti_3AlC_2, Ti_4AlN_3 and Ti_3SiC, Phys. Rev. B, 2000;52:10194.

33. T. Procopio, M. W. Barsoum and T. El-Raghy, Characterization of Ti4AIN3 Met. Mater. Trans. 2000:31A; 333.

34. T. Procopio, T. El-Raghy and M. W Barsoum, Synthesis of Ti4AlN3 and phase equilibria in the Ti-Al-N system. Met. Mater. Trans. 2000:31A; 373.

35. M. W. Barsoum, L. Farber, I. Levin, A. Procopio, T. El-Raghy and A. Berner, High-resolution transmission electron microscopy of Ti_4AlN_3, or $Ti_3Al_2N_2$ revisited J. Am. Cer. Soc. 1999:82; 2545.

36. Onodera A, Hirano H, Yuasa T, Gao N F and Miyamoto Y, Static Compression of Ti_3SiC_2 to 61 GPa Appl. Phys. Letters 1999;74:3782-3784.

37. Barsoum M, Zhen T, Kalidindi S, Radovic M, Murugaiah Fully Reversible Dislocation-based compressive deformation of Ti_3SiC2 to 1GPa Nature Materials, 2003:2;107.

38. Holm B, Ahuja R, and Johannsson B Appl. Phys. Lett. *Ab initio* calculations of the mechanical properties of Ti_3SiC_2 2001;79:10:1450

39. Holm B, Ahuja R, Sa Li and B. Johannsson Theory of the ternary layered system Ti-Al-N Journal of Appl Phys 2002:91; 9874

40. R.Ahuja, O.Eriksson, J.M.Wills, B.Johannsson Appl.Phys.Lett.2000:76; 2226

41. Medvedeva N, Novikov D, Ivanovsky A, Kuznetsov M, and Freeman A, Electronic properties of Ti_3SiC_2 - based solid solutions Phys. Rev B 1998:58; 16042.

42. Z. M. Sun and Y.C. Zhou, Phys. Rev. B, *Ab initio* calculation of titanium silicon carbide (Ti_3SiC_2) 1999:60;1441.

43. X. H. Wang and Y. C. Zhou, Acta Mater., 2002:50; 3141-3149.

44. Pierson H, Handbook of Refractory Carbides and Nitrides, Noyes Pub., Westwood, N.J. 1996.

45. J. Nickl, K. K. Schweitzer & P. Luxenberg, J. Less Common Metals, 1972:26;283.

46. Toulouse J and Launay C Automated system for relative sound velocity and ultrasonic attenuation measurements Rev. Sci. Instrum. 1988;59; 492.

47. G. Alers in Physical Acoustics, Ed. W.Mason Vol IIIB, Academic Press, NY 1965.

48. J. J. Gilman and B. W. Roberts, J. Appl. Phys. 1961:32;1405.

49. R. Chang and L. J. Graham, J. Appl. Phys. 1966:37; 2278.

50. H. J. Frost and M. F. Ashby, Deformation-Mechanism Maps: The Plasticity and Creep of Metals and Ceramics, Pergamon Press, Oxford, 1982.

51. Varshni Y Temperature Dependence of the Elastic Constants Phys. Rev. B, 1970:2:3952.

52. E. S. Fisher and D. Dever, The Science and Technology and Applications of Titanium, Eds. R. I. Jaffe and N. E. Promisel, Pergamon 1968.

53. Blackman M, in Handbuch der Physik, Ed. S. Flugge, Springer Verlag, Berlin 1955.

54. N. W. Ashcroft und N. D. Mermin. Solid State Physics, WB Sounders and Co, 1976.

55. G. Busch and H. Schade, Lectures on Solid State Physics Pergamon Press New York International Series in Natural Philosophy, Gen.Editor: D.Ter Haar 1976;7: 393.

56. V B Krasovitsky, private communications.

57. W. S. Williams, Prog. Solid State Chem.. Eds. H. Riess and J. O. McCladin, 1967:6; 345.

58. J. M. Ziman, Electrons and Phonons, Oxford, London, 1960.

59. A.Ganguly et al unpublished results

60. H.J. McSkimin, In Physical Acoustics, Vol. IA, Ed W.P. Mason, Academic Press, New York :1964; 27-417.

61. Maynard J Resonant Ultrasound Spectroscopy Physics Today June 1996

62. Migliori A et al Phys Rev B Resonance Ultrasonic Spectroscopy Ultrasonic 1990:41;2098

Appendix A: Tables

Table 1. Comparison of elastic properties of Ti_3SiC_2, $TiC_{0.97}$, Ti and Mo.
[a] Calculated from the single crystal data of Fisher and Dever [32], assuming $\mu = \{1/2\ c_{44}\ (c_{12} - c_{12})\}^{1/2}$. The results are extrapolated to room temperature and 0 % Cr content. This table was directly taken form [1] without any correction done later in [2].

Solid	R.T. Young's Mod. (GPa)	R. T. Shear Mod. (GPa)	$d(\mu/\mu_{RT})/dT$ (K^{-1})	Poisson's Ratio	Debye Temp. (K)
Ti_3SiC_2	322 ± 2	133.6 ± 0.8	-1.4×10^{-4}	0.2	427 (this work) 620 (thermal) [19]
$TiC_{0.97}$	456-500 [44,45]	193 [45]	-0.54×10^{-4} [45]	0.18	614 [44]
α–Ti ß-Ti	116 126[a]	43.6 19[a]	 $\approx -1.8 \times 10^{-4}$[a]		420 [52]
Mo	318	122	-1.46×10^{-4} [30]	0.3	470 [50]

Table 2. Summary of results on Ti_3SiC_2 , Ti_4AlN_3 and Ti_3AlC_2 elastic properties obtained in this work [2]. Also listed are previous results on Ti_3SiC_2 [1], [a] this work, fine-grained samples, [b] this work, coarse grained samples, [c] based on results reported in [1] but corrected (see text).

	Ti_3SiC_2	Ti_4AlN_3	Ti_3AlC_2
Room temperature longitudinal velocity, m/s	9100[a] 9142[b] 8950 [c] [1]	8685	8880
Room temperature shear velocity , m/s	5570[a] 5613[b] 5450 [c] [1]	5201	5440
Room temperature mean velocity, m/s	6138[a] 6195[b] 6017[b] [1]	5774	5994
Measured density, g/cm^3	4.47[a] 4.5[b] 4.47 [1]	4.7	4.2
Room temperature Young's modulus, GPa	333 ± 2[a] 339 ± 2[b] 322 ± 2 [c] [1]	310 ± 2	297.5 ± 2
Room temperature shear modulus, GPa	139 ± 2[a] 142 ± 2[b] 133.6± 0.8 [1]	127 ± 2	124 ± 2
Room temperature bulk modulus, GPa	185[a] 187[b] 179 [c] [1] 206 ± 6 [36]	185	165
Poisson's ratio	0.200 ± 0.007[a,b] 0.200 ± 0.007 [c]	0.220 ± 0.007	0.200 ± 0.007
$d(E/E_{RT})/dT$, (K^{-1}) (T > 125 K)	- 0.88 x 10^{-4} [a] - 0.75 x 10^{-4} [b] - 0.95 x 10^{-4} [c] [1]	- 0.74 x 10^{-4}	- 0.84 x 10^{-4}
$d(\mu/\mu_{RT})/dT$, (K^{-1}) (T > 125 K)	- 1.4 x 10^{-4} [a,b] - 1.4 x 10^{-4} [1]	- 1.5 x 10^{-4}	- 1.2 x 10^{-4}
Debye Temperature, K Acoustic Thermal	780[a,b] 784[c] [1] 715 [29]	762 --- 779 [35]	758 --- 764 [35]

Table 3. Summary of the electrical properties of Ti_3SiC_2 determined in this work. Also included are the results for TiC_x and Ti for comparison purposes.

	ρ_{300} $\mu\Omega$ m	$d\rho/dT$ $\mu\Omega$m/K	$R_H \times 10^{11}$ (m^3/C)	$\mu_H \times 10^3$ m^2/(Vs)	p, n x 10^{28} (m^{-3})	Ref.
Ti_3SiC_2	0.22…0.24 0.2273	0.00071 0.00075	+30 ≈ 0	1.6 0.06 to 0.1	< 0.9 14 to 24	[3] [32]
TiC_x	1 to 1.6		-150	0.89 to 1.68	0.37 TO 0.4	[32]
Ti	0.4 to 0.49	0.0017-0.0021	2.8 -.05 to –4.5	0.043 to 0.09	15, 31	[32]

Table 4. Room temperature electric and magneto-electric properties of Ti_3AlC_2 and Ti_4AlN_3 used to calculate the concentration and mobilities of carriers in those compounds. Also included are previous results for Ti_3SiC_2 [1] and TiC_x for comparison purposes.

Compound	ρ 300 K (μΩ-m)	α (m^4/V^2s^2)	R_H $\times 10^{11}$ (m^3/C)	Mobilities (m^2/Vs)		Carrier density (10^{28} m^{-3})	
				μ_n	μ_p	n	p
Ti_3AlC_2	0.387	4×10^{-5}	- 12 ±1	0.0046 to 0.0042	0.0054 to 0.003	0.15 to 0.16	0.2 to 0.4
Ti_4AlN_3	2.61	$\sim 3 \times 10^{-7}$	+ 90±5	_	0.00034	_	0.7
Ti_3SiC_2	0.22	2.06×10^{-3}	+30	0.0023	0.004	0.6	0.6
$TiC_{0.95}$	1 to 1.6		-150 to - 261	0.0012 to 0.0017	–	0.24 to 0.4	–

Table 5. Summary of experimental results and extracted charge carrier concentrations and mobilities for Ti_3AlC_2 as a function of T for various values of b.

T (K)	σ $(M\Omega m)^{-1}$	R_H (10^{11} m^3/C)	α $m^4/(Vs)^2$	$b = \mu_p/\mu_n$	μ_n $m^2/(Vs)$	μ_p $m^2/(Vs)$	n (10^{28} m^{-3})	p (10^{28} m^{-3})
50	5.61	+ 2.2	9×10^{-5}	0.85	0.0086	0.0075	0.17	0.23
				0.60	0.0065	0.0039	0.19	0.56
				0.40	0.0052	0.0021	0.18	1.22
100	5.02	0	8×10^{-5}	0.85	0.0076	0.0065	0.16	0.22
				0.60	0.0059	0.0035	0.17	0.48
				0.40	0.0047	0.0019	0.16	1.03
300	2.61	- 1.2	4×10^{-5}	0.85	0.0046	0.0054	0.15	0.21
				0.60	0.0042	0.0025	0.16	0.38
				0.40	0.0033	0.0013	0.17	0.79

Table 6. The Young's, E , shear, G , and bulk, B, modulii of $Ti_3(Si,Ge)C_2$ obtained from ultrasonic measurements. Also presented is the longitudinal V_l and shear Vs sound velocity measured at room temperature.

Material	B (GPa)	G (GPa)	E (GPa)	V_l (m/s)	Vs (m/s)	Ref
Ti_3SiC_2	180-206	133 - 142	322 - 339	9100	5570	[1,2]
$Ti_3(GeSi)C_2$ for X=0.5	169	131	313	8262	5096	This work
Ti_3GeC_2	148	142	323	7800	5063	This work

Table 7. Room temperature electric properties of $Ti_3(Si,Ge)C_2$ and used to calculate the concentration and mobilities of carriers in those compounds. Also included are previous results for Ti_3SiC_2 , Ti_3AlC_2 [1,2] and TiC_x for comparison purposes.

Compound	ρ (300 K) (μΩ-m)	$d\rho / dT$ (μ Ohm m /K)	α (m^4/V^2s^2)	R_H $\times 10^{11}$ (m^3/C)	Mobilities (m^2/Vs)		Carrier density (10^{28} m^{-3})	
			(T=4K)		μ_n	μ_p	n	p
Ti_3SiC_2	0.255	0.00092	2.06 $\times 10^{-3}$	+30	0.0023	0.004	0.6	0.6
$Ti_3Ge_{0.25}Si_{0.75}C_2$	0.251-0.265	0.00077	-	-	–	–	-	-
$Ti_3Ge_{0.5}Si_{0.5}C_2$	0.273	0.000755	-	-	-	-	-	-
Ti_3GeC_2	0.275	0.000952	1.7 $\times 10^{-3}$	-22	0.0016 to 0.004	0.0016 to 0.004	0.15 to 0.28	0.15 to 0.28
Ti_3AlC_2	0.387	0.000953	4×10^{-5}	- 12 ±1	0.0046 to 0.0042	0.0054 to 0.003	0.15 to 0.16	0.2 to 0.4

Appendix B: Figures

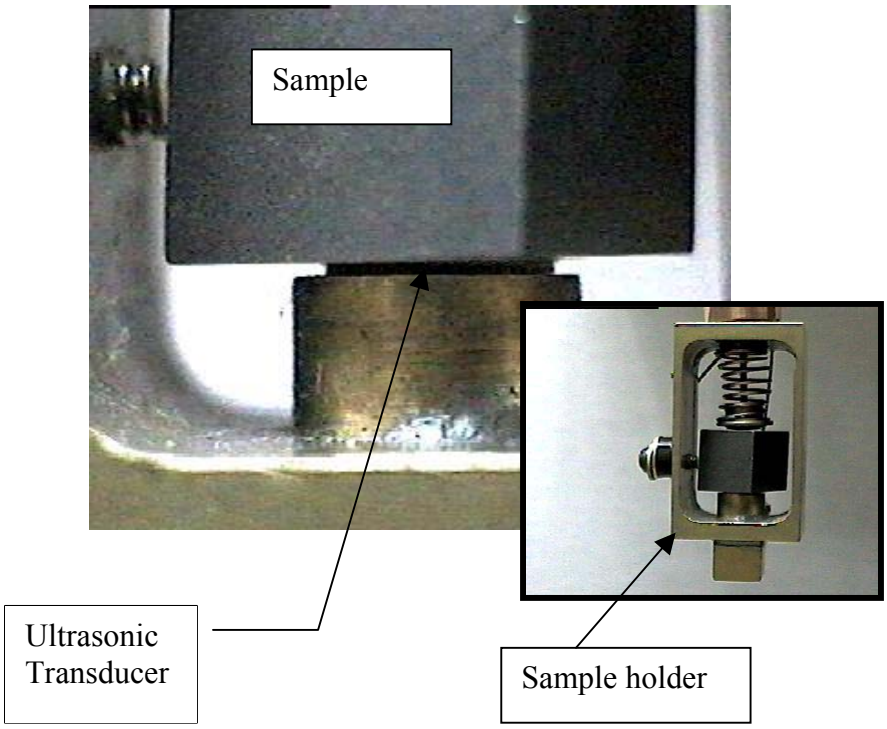

Figure 1. Photograph of the sample and sample holder that used in the ultrasonic velocity measurements setup (Sample holder from [46])

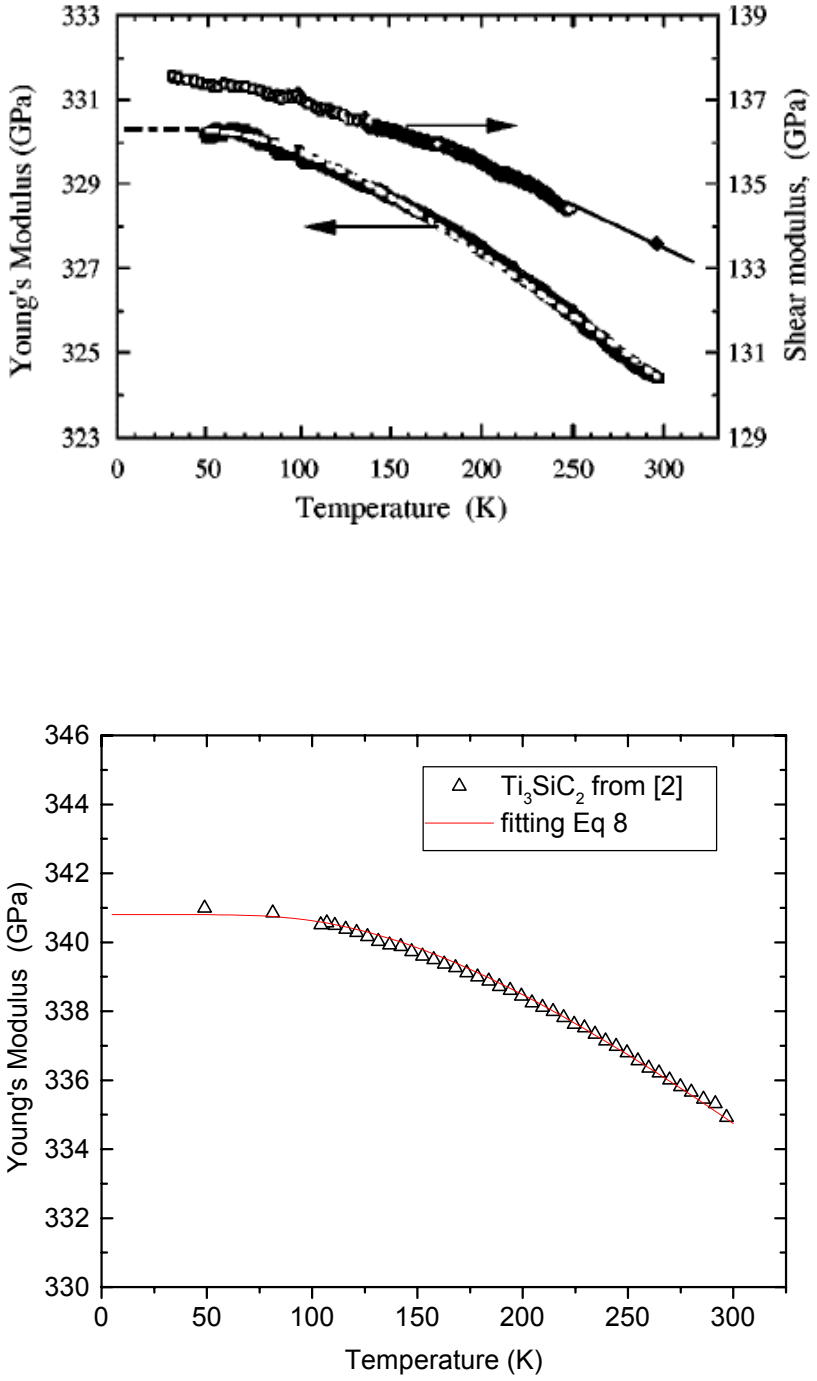

Figure 2. (a)Temperature dependence of Young's and shear moduli of Ti_3SiC_2 in the 20-300K range (sample from [1]); (b) fitting E(T) curve with Eq.8 (sample from [2])

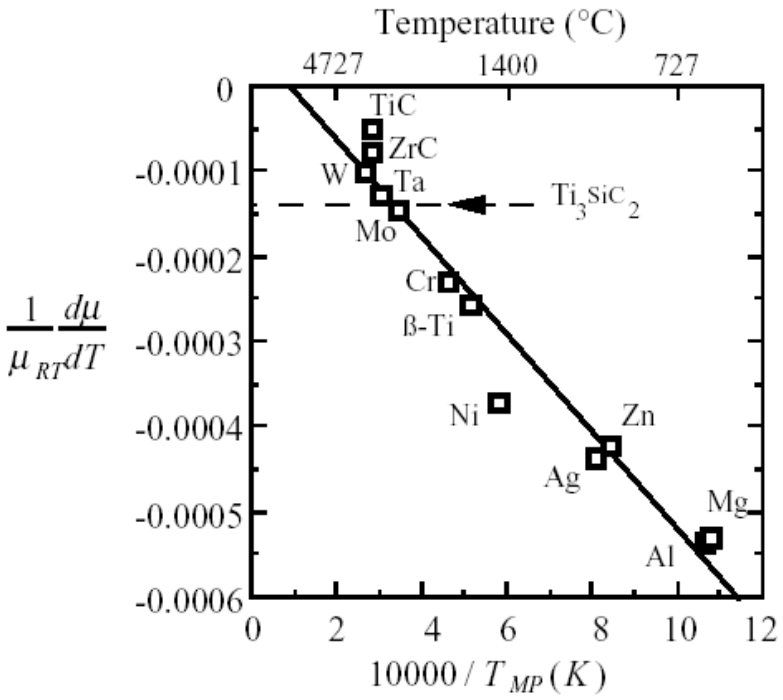

Figure 3. Relationship between $d(\mu/\mu_{RT})/dT$ and the melting points of select elements and compounds.

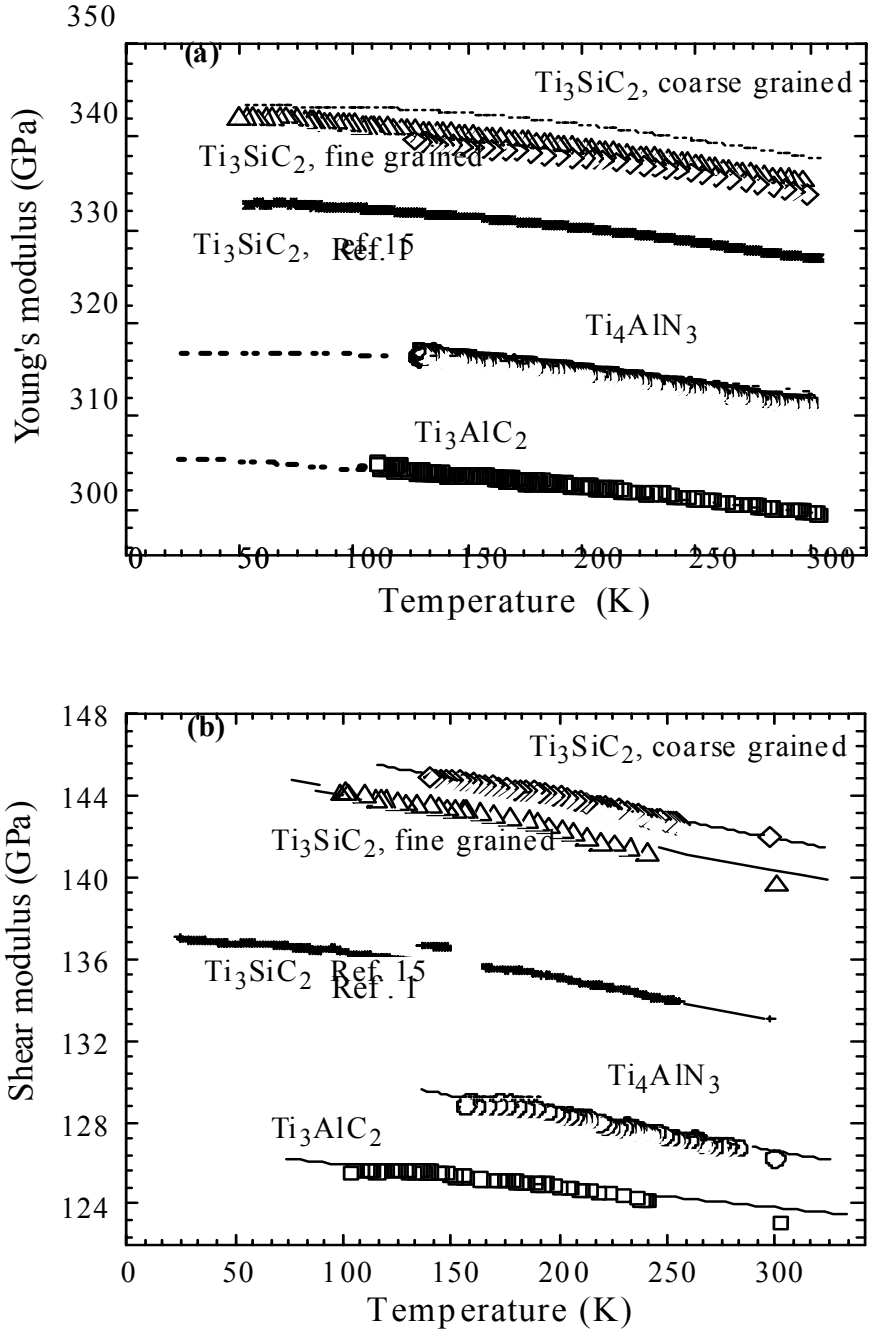

Figure 4. Temperature dependencies of Young's moduli of Ti_4AlN_3, Ti_3AlC_3 and Ti_3SiC_2 in the 30-300 K range. Also included in this figure are our previous results on Ti_3SiC_2. [1]

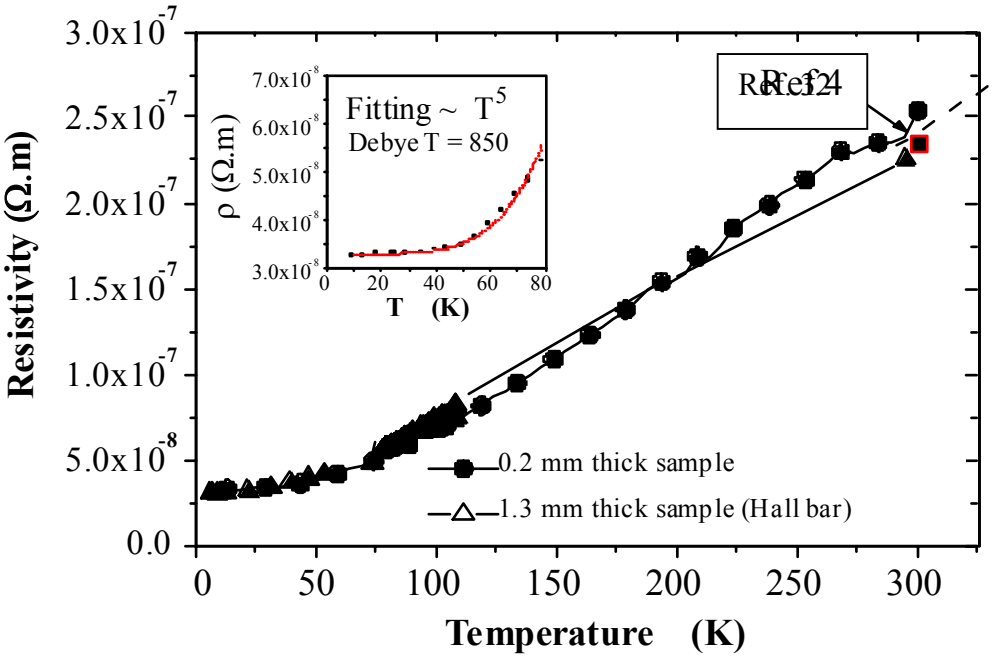

Figure 5. Resistivity versus temperature for several Ti_3SiC_2 samples, insert - low temperature resistivity fitting using Bloch formula.

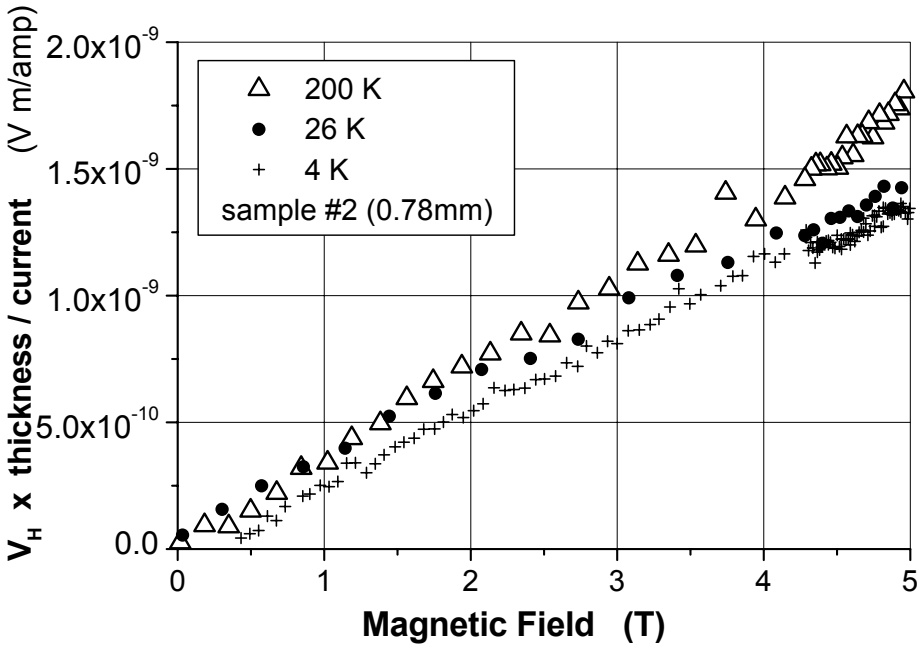

Figure 6. Hall voltage as a function of the magnetic field for various temperature

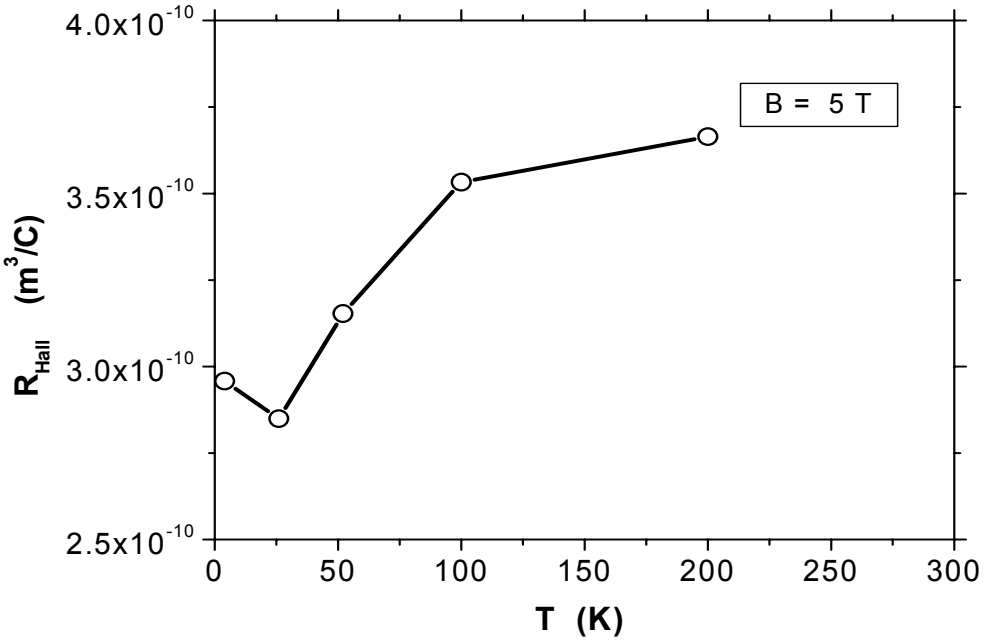

Figure 7. Hall coefficient as a function of temperature for B= 5T

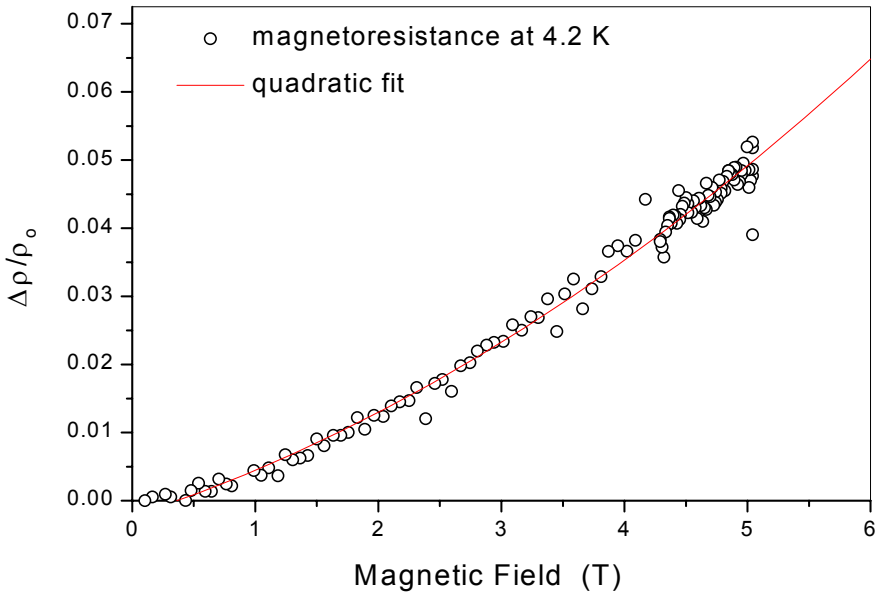

Figure 8. Magnetoresistance of Ti_3SiC_2 as a function of magnetic field.

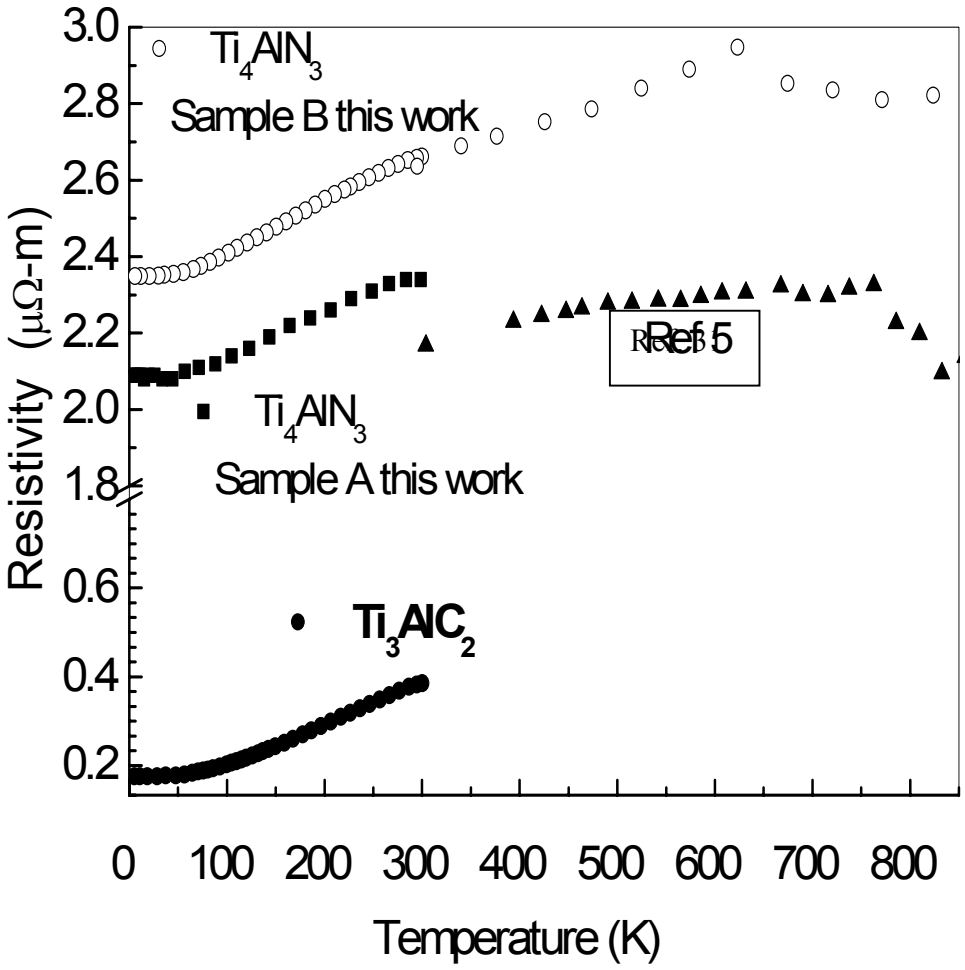

Figure 9. Plot of the resistivity versus temperature for Ti_3AlC_2 and Ti_4AlN_3. Note the large residual resistivity of Ti_4AlN_3 and the difference in scale. The room temperature resistivity of Ti_4AlN_3 is nearly an order of magnitude larger than that of Ti_3AlC_2. The data are plotted for two samples of Ti_4AlN_3: the one measured in this work (sample B) and another one from [31] (sample A). This shows agreement with high temperature transport data from [31].

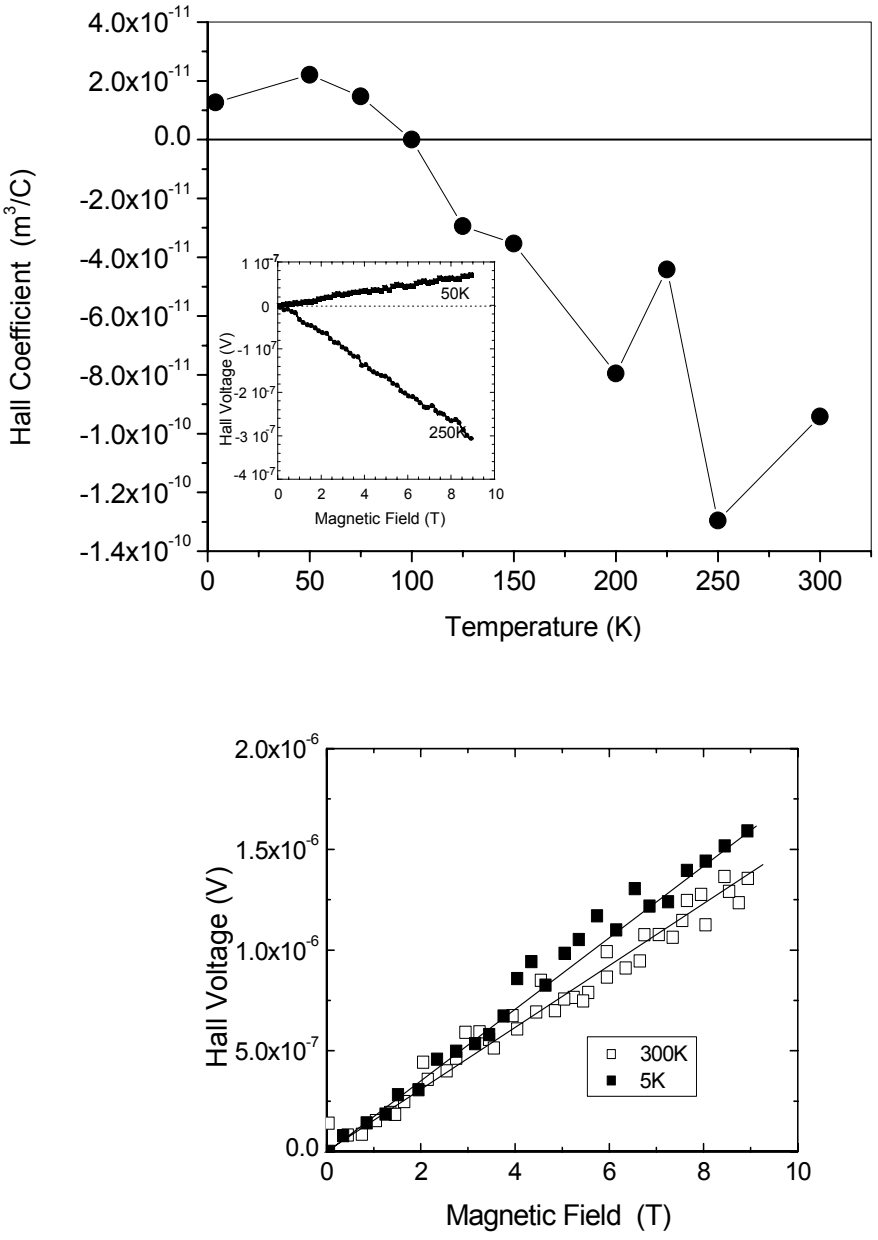

Figure 10. Temperature dependence of the Hall coefficient for Ti_3AlC_2. Inset: Field dependence of V_H. (a) V_H as a function of B for Ti_4AlN_3 at various temperatures. (b)

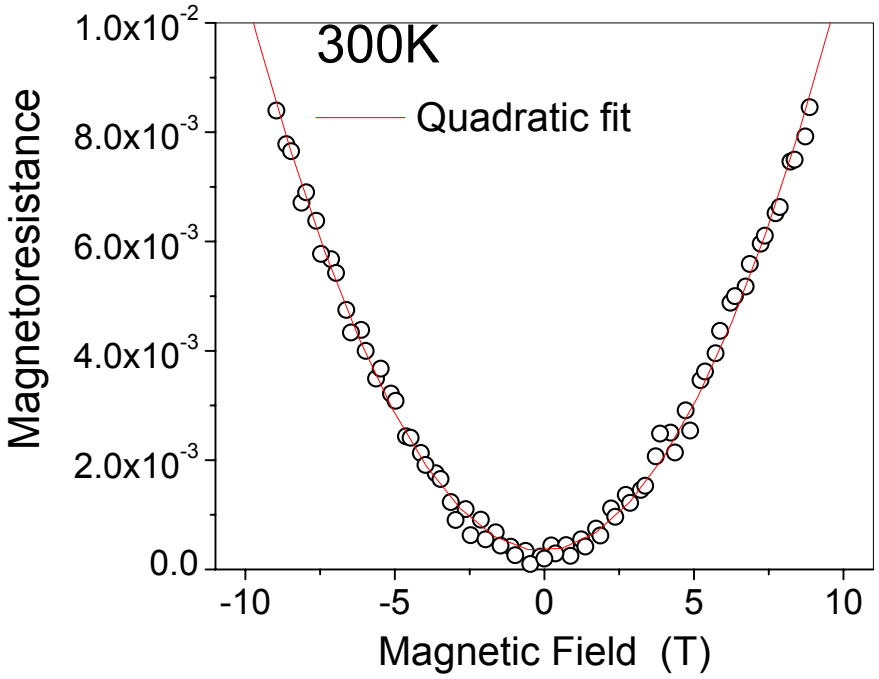

Figure 11. Field dependence of the magnetoresistance of Ti_3AlC_2 at 300 K.

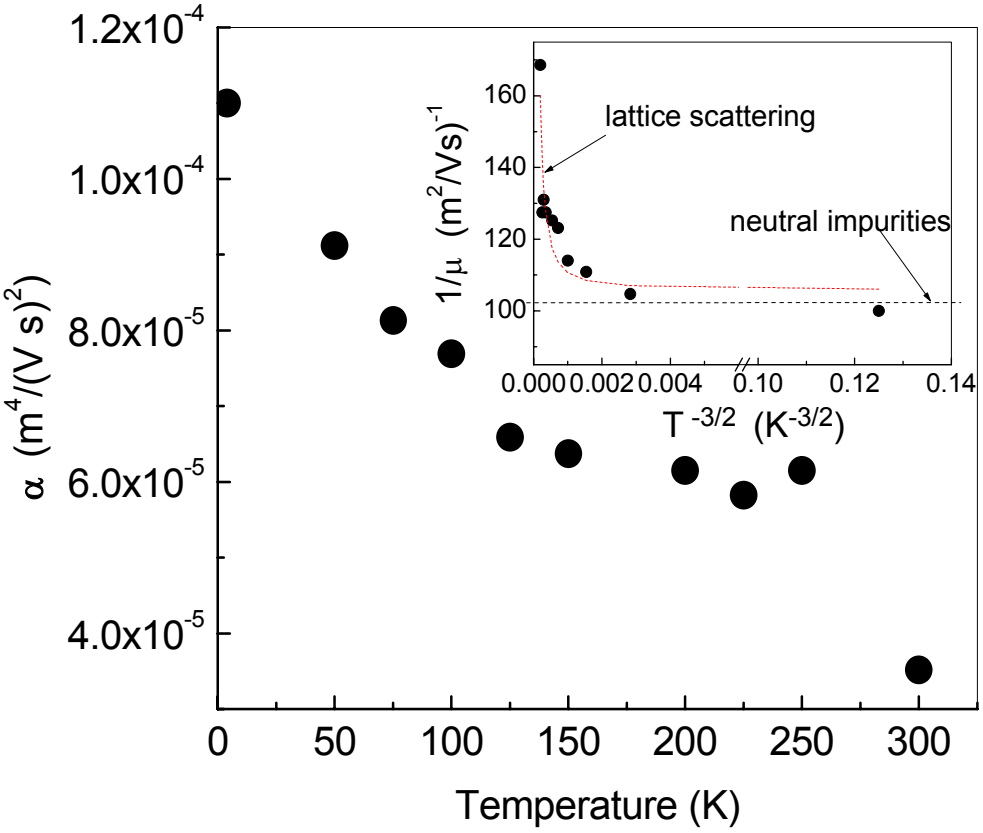

Figure 12. Temperature dependence of the magnetoresistance prefactor α for Ti_3AlC_2. Inset: temperature dependence of the inverse mobility vs. $T^{-3/2}$. The neutral impurities dominate at low T; lattice scattering becomes important at higher temperatures.

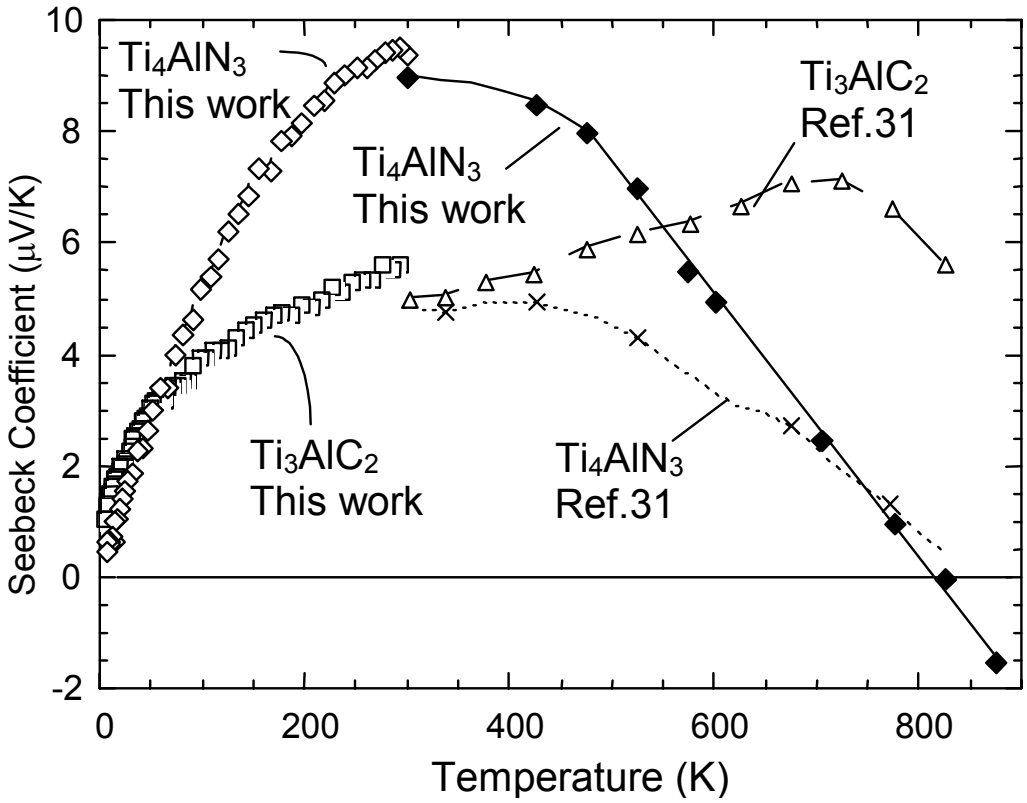

Figure 13. Seebeck coefficient versus temperature for Ti_3AlC_2 and Ti_4AlN_3. Also included are previous results. Note: the low-temperature results were obtained at Rowan and the high-temperature ones were measured in Korea (sample B), which was different from sample A used in [31] and for which the conductivity is shown in Fig. 8.

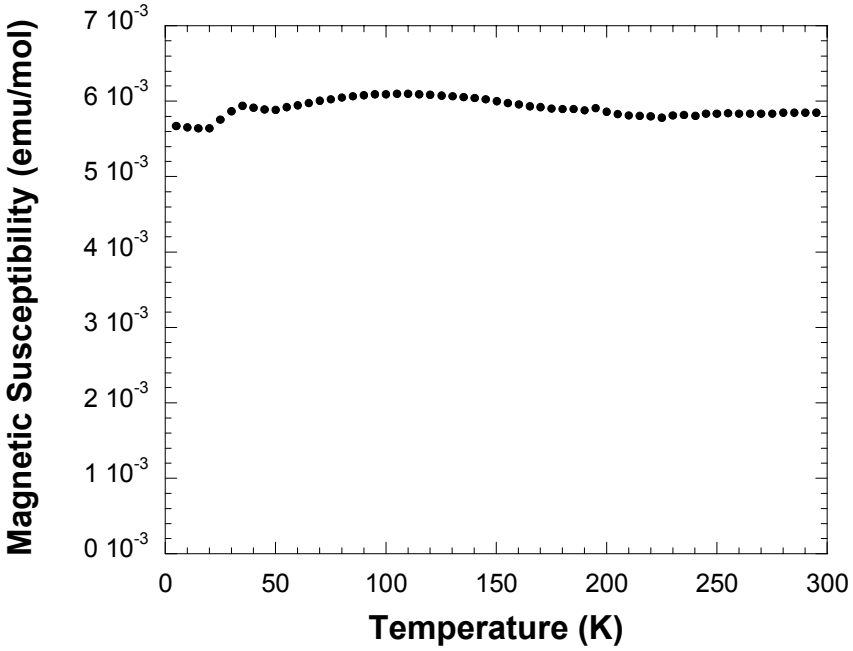

Figure 14. Magnetic susceptibility of Ti_3AlC_2 as a function of temperature. Note that it is constant aside from a weak maximum near 100 K.

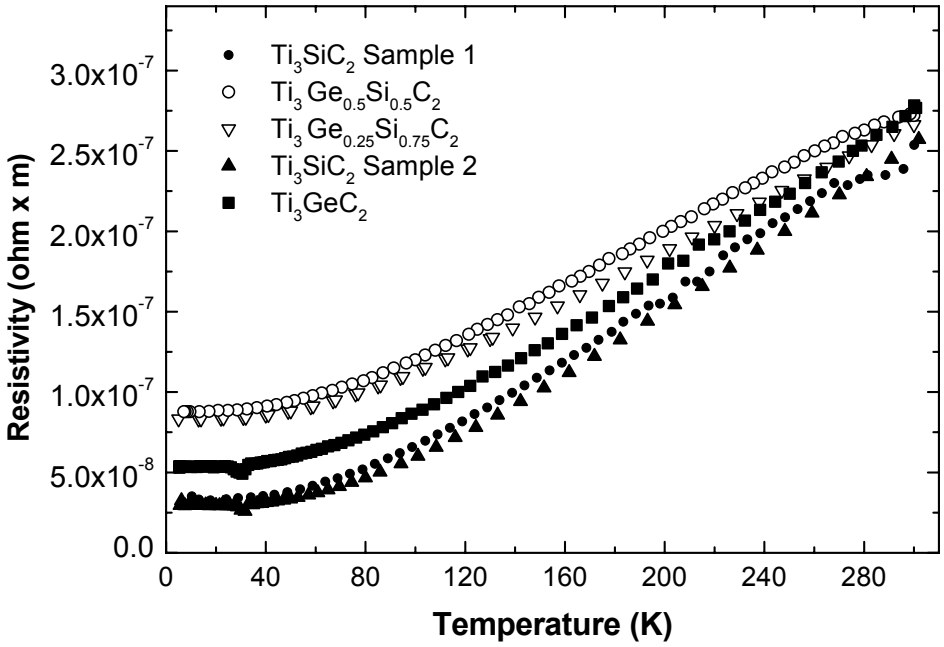

Figure 15. Resitivity as a function of temperature for $Ti_3(SiGe)C_2$ phases

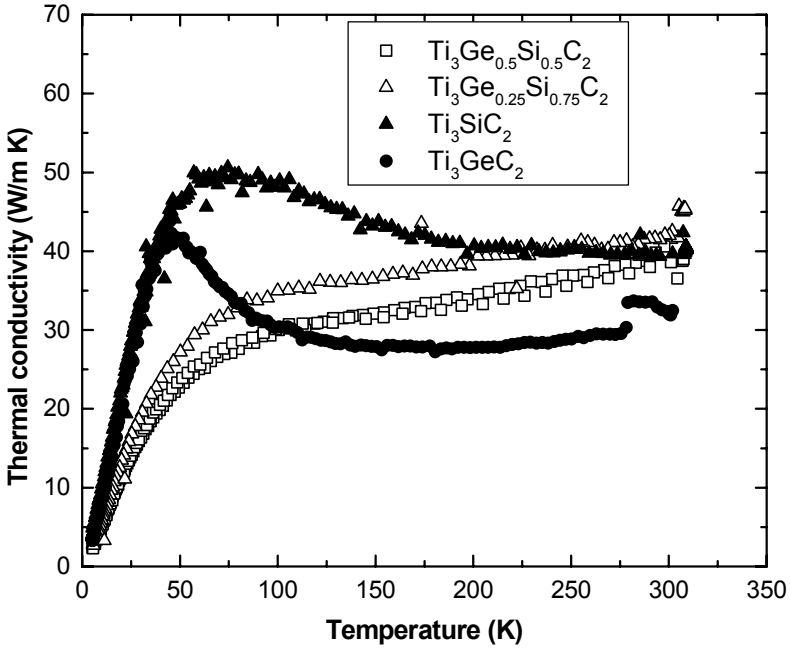

Figure 16. Thermal conductivity as a function of temperature for $Ti_3(SiGe)C_2$ phases

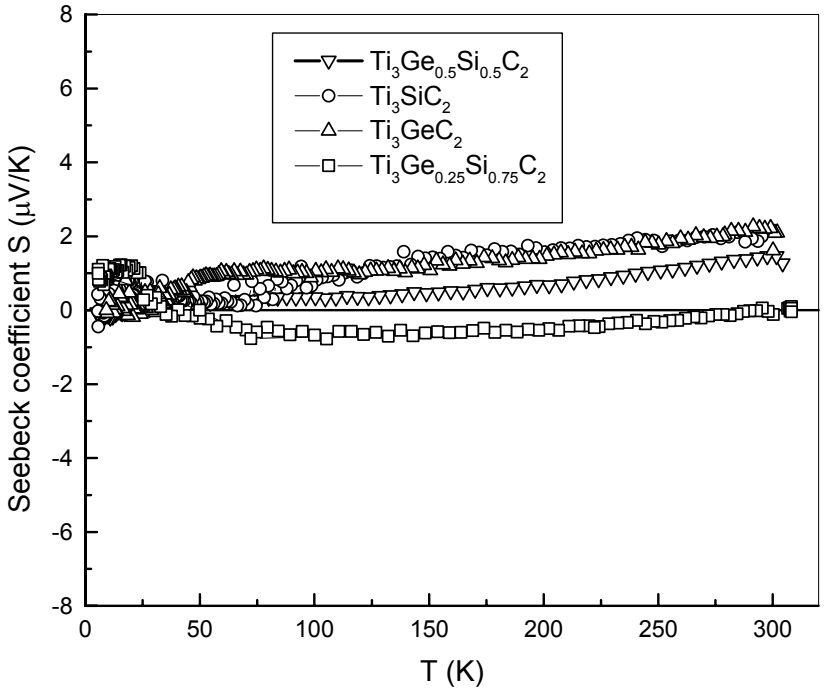

Figure 17. Seebeck coefficient as function of temperature for $Ti_3(Si,Ge)C_2$

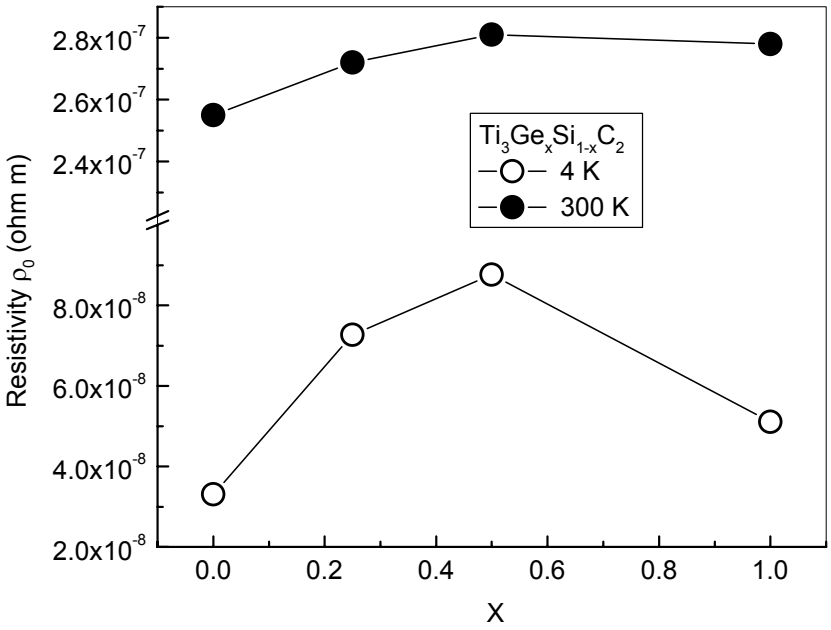

Figure 18. Residual and room temperature resistivity as function of Ge composition in for $Ti_3(Si,Ge)C_2$

Appendix C: Experimental Ultrasonic Technique Review

Elastic Constants Measurements Using Ultrasonic Method

The elastic constants are one of the fundamental parameters to be evaluated. Thermodynamically, the elastic constants are defined by the shape of the interatomic bonding energy in the vicinity of the minimum. Therefore, any changes in crystal structure or electronic character of materials are often revealed through the changes in the elastic properties. It is clear that accurate measurements of the elastic constant, especially, as a function of temperature, provide significant information about the material. To measure the elastic constants of a material there are three commonly used methods which are based on: 1) measuring of the slope of stress-strain curve, 2) propagation of ultrasonic waves speed measurements or 3) dynamic resonance or natural vibration frequency measurements.

The first one, based on static tension load testing, is very simple in concept (wich measures the displacement as a function of the applied load). However, its approach can be difficult to achieve experimentally. When applied to ceramics or other very stiff materials, conventional tension testing will be problematic and cumbersome due to the problem related to specimen grip and alignment. In addition, very small resultant strains can be difficult to measure. Often destructive, this method suffers from a vast number of experimental errors.

As has been established for a long time, the easiest technique to measure elastic constant is the one that uses a propagating sound wave. This approach is based on measurements of the time of flight, *t* (or round-trip transit time*)* of elastic

waves in the material in order to obtain the sound velocity, V from V= 2L/*t* , where L is the specimen length. When applied to the isotropic materials, the elastic constants can be obtained from the longitudinal V_l and transverse (shear) V*s* ultrasonic wave velocities (see Chapter 2). So far, the most accurate, precise and complete set of elastic constants has been determined by measuring the time of flight of sound pulse.

Recently Resonance Ultrasonic Spectroscopy (RUS) technique [61,62] has emerged. It is based on dynamic resonance approach when a specimen vibrates at its fundamental frequency using the (standing waves wavelength are twice length of specimen). By measuring the resonance spectra, one can quantify elastic properties by solving the wave equation for particular configurations. This procedure can be complex, but basically, knowledge of the specimen dimensions, density and fundamental vibration frequency allow the elastic constants to be determined. The mode of vibration determines which of the elastic constants can be measured. This technique provides very accurate results, however, often requires specially parallelepiped (or cylindrical) shaped and polished samples, as well as rather tedious and sophisticated resonance peaks fitting procedure.

In our work we chose the second technique utilizing ultrasonic echo pulses time of flight measurements, even though this method demands at least two measurements of the ultrasonic velocities (longitudinal and shear), and relatively large samples. When carried out on polycrystalline specimen (such as ceramics, metals), this technique allowed us to get good results using a relatively simple commercially available apparatus. The echo-pulse time of flight phase-sensitive

method developed in [60] is one of the most commonly used technique to measure the velocity of sound in solids, because of its precision of 2 ppm and capability to be automated. The principle of the phase sensitive technique is in the measurements of the phase ϕ of a given echo relative to the reference echo. This phase (or its change) can be obtained from $\phi = \tan^{-1}(V_1/V_2)$ by measuring in-phase component of the given echo amplitude V_1 and its quadrature component amplitude V_2. Then the time *t* between two echoes (reflected and a reference tone burst) is a simple function of the phase of the signal and the frequency of the tone–burst, *f*: $t = \phi / 2\pi f$. The ultrasonic setup is nothing more than a superheterodyne receiver circuitry similar to that used in standard radio receivers. The system includes two phase-sensitive detectors (operating at the intermediate frequency) wherein the references are at the same frequency but shifted by 90 degrees with respect to each other. This allows the acquisition of the real and imaginary parts of the received signals. Gated integrators then act on a selected signal, and the resultant dc voltages V_1 and V_2 are recorded by the computer (via data acquisition analog to digital card) for measurement purposes.

Temperature dependence of ultrasonic velocities was determined in this work by measuring of the time difference between consequent echoes produced by a piezoelectric transducer mounted on the specimen. The specimens for this study were machined as a rectangular prism/parallelepipeds with flatness and parallelism of the surface better than 3 microns. Quartz or lithium niobate crystal with fundamental frequencies 5, 10 or 15 MHz were used as transducers. Transducers were mounted on the specimen using phenyl salicilate (Salol) as a bonding agent. To produce longitudinal and shear waves X-cut and Y-cut transducers were used,

For a transit time of 2-3 μs the best resolution in velocity was 10^{-5} . Typically, error in density bring overall elastic constant error to roughly 0.05%.

The effect of the microstructure and anisotropy were studied by varying the measurement frequency between 5-20MHz. This frequency variation did not affect the time of flight (and the measured velocity). This implies that any dispersion effects are very small and could be neglected. Thus the elastic constants measured at high frequencies can be considered to be equal to a static modulii.